RESEARCH MEMORANDUM

INVESTIGATION AT HIGH SUBSONIC SPEEDS OF THE EFFECTS OF VARIOUS UNDERWING EXTERNAL-STORE ARRANGEMENTS ON THE AERODYNAMIC CHARACTERISTICS OF A 1/16-SCALE MODEL OF THE DOUGLAS D-558-II RESEARCH AIRPLANE

By H. Norman Silvers and Thomas J. King, Jr.

Langley Aeronautical Laboratory
Langley Field, Va.

NATIONAL ADVISORY COMMITTEE
FOR AERONAUTICS
WASHINGTON
July 18, 1955

NACA RM L55D11

[redacted]

NATIONAL ADVISORY COMMITTEE FOR AERONAUTICS

RESEARCH MEMORANDUM

INVESTIGATION AT HIGH SUBSONIC SPEEDS OF THE EFFECTS OF VARIOUS UNDERWING EXTERNAL-STORE ARRANGEMENTS ON THE AERODYNAMIC CHARACTERISTICS OF A 1/16-SCALE MODEL OF THE DOUGLAS D-558-II RESEARCH AIRPLANE

By H. Norman Silvers and Thomas J. King, Jr.

SUMMARY

An investigation was made at high subsonic speeds of various arrangements of underwing external stores on a 1/16-scale model of the Douglas D-558-II research airplane. In each configuration, two stores were located symmetrically from the plane of symmetry at 0.61 semispan. Three sizes of a short-cylinder shape and two sizes of a long-cylinder shape were investigated. Three thicknesses of the pylon support were investigated on one store configuration. The free-stream thickness ratios ranged from 7.6 percent to 4.2 percent of the pylon chord.

The results of this investigation indicated that increasing the store size increased the total model drag by as much as 97 percent at a Mach number of 0.94; but the increase in store volume with store size was such as to result in a decrease in installation drag per unit volume. At the high Mach numbers the long-cylinder and short-cylinder stores produced about the same installation drag. Considerable reduction in installation drag came from a reduction in pylon thickness ratio at all Mach numbers, except those near the upper test limit ($M = 0.96$), where the effect of pylon thickness was inconclusive. The stores increased the lift-curve slopes and decreased the stability of the model at low lift coefficients and tended to reduce the adverse effects of pitch-up of the model.

INTRODUCTION

One item of considerable interest to designers of high-speed service aircraft concerns the ability of the aircraft to carry external fuel

[redacted]

tanks or stores through the operational speed range. Many uncertainties exist in connection with both the effects of external stores on the general behavior of the airplane and more specifically on ways to reduce the drag penalties imposed by store installations. To obtain information on these problems, the National Advisory Committee for Aeronautics is conducting investigations on the Douglas D-558-II research airplane. The program includes wind-tunnel tests of various store configurations at subsonic, transonic, and supersonic speeds at the Langley Aeronautical Laboratory and flight tests of the airplane with selected store configurations at the NACA High-Speed Flight Station, Edwards, Calif. In reference 1 are presented the results of an investigation at supersonic speeds. The present paper presents some tunnel results of an investigation to evaluate store-installation drag on a 1/16-scale model of the D-558-II airplane at subsonic speeds. Results were obtained as functions of angle of attack and Mach number, the maximum Mach number being 0.96. Some results of wind-tunnel tests at transonic speeds of the same model (with the exception of a few minor details) without stores are presented in reference 2.

SYMBOLS

C_L lift coefficient, $\frac{\text{Lift}}{qS}$

C_D drag coefficient, $\frac{\text{Drag}}{qS}$

C_m pitching-moment coefficient, $\frac{\text{Pitching moment}}{qS\bar{c}}$

C_{D_B} base drag coefficient, $\frac{P_B - P}{q}\frac{S_B}{S}$

ΔC_D installation-drag coefficient, $C_{D_{\text{model+stores}}} - C_{D_{\text{model}}}$

C_{D_V} installation-drag coefficient based on stores volume, $\Delta C_D \left(\frac{S}{V_S^{2/3}}\right)$

q free-stream dynamic pressure, $\frac{1}{2}\rho V^2$, lb/sq ft

P_B pressure at the base of the fuselage, lb/sq ft

P free-stream static pressure, lb/sq ft

V free-stream velocity, ft/sec

ρ mass density of air, slugs/cu ft

S wing area, 0.684 sq ft

S_B fuselage base area, 0.0132 sq ft

$\bar{c}$ mean aerodynamic chord of wing, 0.455 ft, $\frac{2}{S}\int_0^{b/2} c^2 dy$

c local wing chord parallel to free stream

V_S volume of both stores, cu ft

d diameter of stores, ft

R Reynolds number

M Mach number

α angle of attack referred to fuselage reference line, deg

i_t incidence of the horizontal tail referred to fuselage reference line, positive when leading edge is raised, deg

$$C_{L_\alpha} = \frac{\partial C_L}{\partial \alpha}$$

$$C_{m_{C_L}} = \frac{\partial C_m}{\partial C_L}$$

$$\Delta\left(C_{L_\alpha}\right) = \left(C_{L_\alpha}\right)_{\text{model+stores}} - \left(C_{L_\alpha}\right)_{\text{model}}$$

$$\Delta\left(C_{m_{C_L}}\right) = \left(C_{m_{C_L}}\right)_{\text{model+stores}} - \left(C_{m_{C_L}}\right)_{\text{model}}$$

[redacted]

MODEL AND APPARATUS

A three-view drawing of the model, along with a tabulation of the geometric characteristics is presented in figure 1. Photographs showing the model with one arrangement of stores in the Langley high-speed 7- by 10-foot tunnel are presented in figure 2.

The model used in the tunnel investigations (refs. 1, 2, and herein) was the same basic model, although some differences exist between the original configuration of the model in reference 2 and the configuration tested in reference 1 and herein. The configuration of reference 2 did not have a canopy and it had a vertical tail of reduced span. The span of the vertical tail of the present configuration is scaled from that used on the airplane. There are some differences between the present model and the airplane. They include an enlarged aft portion of the model fuselage to allow attachment of a sting support, and a model wing-tip-thickness ratio of 10 percent instead of 12 percent.

Details of the external stores investigated are presented in figure 3. Each store installation consisted of two identical stores located symmetrically from the plane of symmetry at 0.61 semispan. The store installations consisted of two shape series (ordinates in table I) that were scaled to produce three sizes of one shape (designated stores A, B, and C) and two sizes of the other (designated stores D and E). The shape of stores A, B, and C, which will be referred to as the short-cylinder shape, is a shape developed by the Douglas Aircraft Company, Inc., and is frequently referred to as the DAC store shape. The shape of stores D and E, which will be called the long-cylinder shape, was developed by the Wright Air Development Center and is frequently referred to as the WADC store shape. The stores and the store fins using the short-cylinder shape are 1/16-scale models of a full-scale 1,000-pound bomb (store A), a 2,000-pound bomb (store B), and a 150-gallon fuel tank (store C). The fins used on the long-cylinder stores are identical with those used on short-cylinder stores of the same length. The fins on all stores were at 45° to the horizontal and the vertical. The lengths of the long-cylinder stores were made to correspond to those of the short-cylinder stores (stores A and C correspond in length to stores D and E, respectively), but because of a somewhat larger diameter and different profile development, the long-cylinder shape had a greater displacement for the same length.

The details of the pylons investigated are presented in figure 4. The pylons were identical in sweep and chord length, but not in the cross-section profile. The pylons are identified by their streamwise thickness ratios as the 7.6-percent pylon, the 6.2-percent pylon, and the 4.2-percent pylon. All the pylons had parallel-sided midchord sections. The 7.6-percent pylon had a shorter parallel-sided section than either the

6.2- or the 4.2-percent pylons. The thickness distributions of the 6.2- and 4.2-percent pylons differed only by a constant factor. Ordinates of the pylons are given in figure 4. All pylons were hand filed to the ordinates shown.

Force and moment measurements were obtained from a six-component strain-gage balance located within the fuselage. The model-balance combination was supported by a sting mounting system (fig. 2) that attached to the balance through the base of the fuselage.

TESTS AND ACCURACY

The tests were made in the Langley high-speed 7- by 10-foot tunnel at Mach numbers from 0.40 to 0.96. Two types of tests were made in this investigation. One type was made at constant Mach numbers through an angle-of-attack range. The results of these tests were used primarily to establish the lift and pitching-moment characteristics of the model. The second type of test was made at a constant angle of attack ($\alpha = -2^\circ$) through a Mach number range. Previous experience has indicated that this type of test gives the more reliable drag characteristics of the model. An angle of attack of -2° corresponds approximately to the angle of attack for zero lift of the model without stores.

In evaluating the various external-store installations, the drag coefficients are of primary importance. The repeatability of the drag measurements obtained at $\alpha = -2^\circ$ for various Mach numbers have consequently been estimated and are listed below for several Mach numbers.

M	C_D
0.40	±0.0026
-.70	±.0010
-.85	±.0008
-.94	±.0007
-.96	-------

No values are presented for $M = 0.96$ because certain factors affecting the repeatability of data at this Mach number are not quantitatively known. They include proximity to tunnel choking and uncertainties of fairing that portion of a drag curve where the values are increasing rapidly. The drag characteristics of the model at constant Mach numbers through the angle-of-attack range are presented, but they are not considered accurate enough (especially at the higher Mach numbers) for comparison with the drag measurements obtained at $\alpha = -2^\circ$ and various Mach numbers.

The variation of test Reynolds number with Mach number is presented in figure 5.

CORRECTIONS

Blocking corrections applied to Mach number and dynamic pressure were determined by the method of reference 3. Jet-boundary corrections were calculated by the method of reference 4 and were applied to the angle of attack and drag. Jet-boundary corrections to the pitching-moment coefficients were considered negligible and were not applied.

The angles of attack have been corrected for deflection under load of the sting support system and the strain-gage balance. No tare corrections have been made to these results for the effect of the sting support on the external surfaces near the base of the model. However, the drag coefficients have been adjusted to correspond to coefficients where the pressure at the base of the fuselage is equal to free-stream static pressure. The average base drag coefficients are presented in figure 6. These values were about the same for all store-on configurations of the model. The base drag coefficient increments have been added to the drag coefficients to obtain the results presented in this paper.

RESULTS AND DISCUSSION

The results obtained throughout the pitch range at various Mach numbers are presented in figure 7 for the model without stores and in figures 8 to 16 for the model with the various external-store arrangements. In figures 17, 18, and 19 the drag characteristics of the model with the various store arrangements are presented as a function of Mach number at an angle of attack of -2°. The effects of pylon thickness ratio and store size on the drag characteristics at $\alpha = -2^{\circ}$ are summarized in figures 20 and 21. The effects of store size on the lift-curve and pitching-moment curve slopes (taken at zero lift) are summarized in figure 22.

In the figures presenting the results as a function of lift coefficient (figs. 7 to 16) solid symbols are shown at zero lift for each Mach number. These symbols represent the intersection of the reference axes corresponding to the particular Mach numbers.

Drag Characteristics

Without the external stores on the model, it is seen that the lowest drag coefficient of the model is about 0.0130 (fig. 17). This value compares fairly well with the model drag coefficient (about 0.0150) reported in an earlier investigation (ref. 2). The effect of the horizontal tail on the drag coefficient is shown with the store arrangement in place (fig. 17). The horizontal tail at $i_t = 0^\circ$ results in a minimum increase in drag coefficient of about 0.0040, and at $i_t = -2^\circ$ about 0.0100. These values of drag coefficient due to the horizontal tail also agree well with the drag contribution of the horizontal tail indicated in reference 2.

The effect of pylon thickness ratio on the drag characteristics at $\alpha = -2^\circ$ with stores A in place (fig. 18) indicates that reducing the pylon thickness reduces the installation drag coefficient. The reduction is illustrated in figure 20, where the results of figure 18 are cross-plotted for selected Mach numbers. At a Mach number of 0.60, a reduction of thickness from 7.6 to 4.2 percent reduced the installation-drag coefficient about 43 percent. Similar reductions occur at Mach numbers up to about $M = 0.92$ (fig. 18). At the higher Mach numbers there appear to be no drag advantages in reducing pylon thickness ratio.

The effect of store size on the installation drag coefficients is shown in figure 21. These results were obtained by cross-plotting the results of figure 19. The volume against which the installation drag coefficient is plotted is the total displacement volume at full-scale of the two store shapes making up the installation. The results show an increase in installation drag with increase in store size (fig. 21(a)). The increase in installation drag becomes greater as the Mach number increases. At $M = 0.94$ the smallest short-cylinder stores (store A) and the largest stores (store C) increased the total drag by about 46 percent and 97 percent, respectively (see fig. 19). This increase in stores size from the small short-cylinder stores to the large stores resulted in an increase in installation drag of about 83 percent. The results (fig. 21(a)) also show that at the lower Mach numbers the stores with the long-cylinder shape produced less installation drag at a given volume than the short-cylinder shape. To obtain a quantitative conception of the effect of store volume, the installation drag coefficients have been converted to a volume basis and the results are presented in figure 21(b). The results show that in general the installation drag coefficients based on store volume show some decrease with increase in store volume. At the lowest Mach numbers there is a distinct drag advantage to the stores with the long-cylinder shape; however, at the high Mach numbers the long- and the short-cylinder shape stores, in general, produced about the same total installation drag as well as drag per unit of store volume.

Lift and Pitch Characteristics

The effect of store size and shape on the lift-curve and pitching-moment curve slopes are summarized in figure 22. All arrangements of stores increase the lift-curve slope and produce a destabilizing change in the aerodynamic-center location. At the higher Mach number (M = 0.94) the change in the aerodynamic-center location is large enough to be worthy of consideration. The long-cylinder shape is more destabilizing than the short-cylinder shape and instability of both shapes increases with increase in store volume. The largest stores (store E) of the long-cylinder shape produce a rearward movement of the aerodynamic center of about 9 percent of the mean aerodynamic chord.

It is also of interest to examine the pitching-moment curves with respect to pitch-up. The model without stores and having $i_t = 0^\circ$ has very little stability at lift coefficients of about 0.6 (fig. 7). At lift coefficients slightly above 0.6, a break in the pitching-moment curve exists that is known to result in undesirable airplane behavior of a type referred to as pitch-up. Comparing these data with results obtained with stores A and the 7.6-percent pylons for the same stabilizer setting (fig. 8(b): the only set of data with complete Mach number range) shows that the store arrangement has a tendency to reduce the pitch-up break in the pitching-moment curves. The results are not as conclusive for the other arrangements of stores. It does, however, appear that, in general, the other stores may delay to higher lift coefficients the pitch-up break in the pitching-moment curves.

CONCLUSIONS

An investigation at high subsonic speeds of the effects of various underwing external store arrangements on the aerodynamic characteristics of a 1/16-scale model of the Douglas D-558-II research airplane indicates the following conclusions:

1. Increasing the store size over the range of sizes investigated increased the total model drag by as much as 97 percent at Mach number of 0.94. In general, the increase in store volume was such as to result in a decrease in drag per unit volume as the store size increased. The long-cylinder stores produced less drag than the short-cylinder stores at low Mach numbers, but both long-cylinder and short-cylinder stores gave about the same installation drag increases at the higher Mach numbers.

2. Reducing the thickness ratio of the pylon support member of the external store installation from 7.6 percent to 4.2 percent reduced the drag due to installation considerably at all Mach numbers, except those near the upper test limit (M = 0.96), where the effect of the pylon thickness was not conclusive.

[redacted]

3. The external stores increased the lift-curve slopes of the model and reduced the stability of the model at low lift coefficients. At the higher lift coefficients the stores tended to reduce the adverse effects of pitch-up of the model.

Langley Aeronautical Laboratory,
National Advisory Committee for Aeronautics,
Langley Field, Va., March 23, 1955.

REFERENCES

1. Smith, Norman F.: Exploratory Investigation of External Stores on the Aerodynamic Characteristics of a 1/16-Scale Model of the Douglas D-558-II Research Airplane at a Mach Number of 2.01. NACA RM L54F02, 1954.

2. Osborne, Robert S.: High-Speed Wind-Tunnel Investigation of the Longitudinal Stability and Control Characteristics of a 1/16-Scale Model of the D-558-II Research Airplane at High Subsonic Mach Numbers and at a Mach Number of 1.2. NACA RM L9C04, 1949.

3. Hensel, Rudolph W.: Rectangular-Wind-Tunnel Blocking Corrections Using the Velocity-Ratio Method. NACA TN 2372, 1951.

4. Gillis, Clarence L., Polhamus, Edward C., and Gray, Joseph L., Jr.: Charts for Determining Jet-Boundary Corrections for Complete Models in 7- by 10-Foot Closed Rectangular Wind Tunnels. NACA WR L-123, 1945. (Formerly NACA ARR L5G31.)

Table I

Store ordinates

(percent of store length)

Short-cylinder shape
(Stores A, B, C)

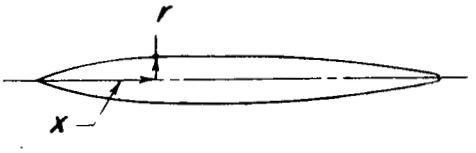

x	r
0	0
1.95	0.95
4.72	2.03
7.51	2.88
10.29	3.52
15.85	4.43
21.40	5.04
26.93	5.49
29.73	5.67
32.53	5.80
35.33	5.84
Straight line	
49.73	5.84
52.53	5.81
55.33	5.76
60.93	5.51
66.40	5.13
72.00	4.63
77.60	4.03
83.20	3.35
88.66	2.63
93.73	1.95
96.00	1.63
98.13	1.28
100.00	0
T.E.R.	0.56

Long-cylinder shape
(Stores D, E)

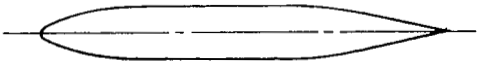

x	r
0	0
1.11	1.88
2.23	2.62
3.35	3.17
4.47	3.63
5.57	4.01
6.71	4.35
8.93	4.84
14.49	5.79
17.28	6.07
20.08	6.28
21.43	6.37
23.37	6.40
25.69	6.44
Straight line	
61.47	6.44
63.60	6.40
64.80	6.37
67.07	6.28
70.00	6.07
72.67	5.79
78.40	4.85
79.20	4.72
Straight-line taper	
100.00	0

[redacted]

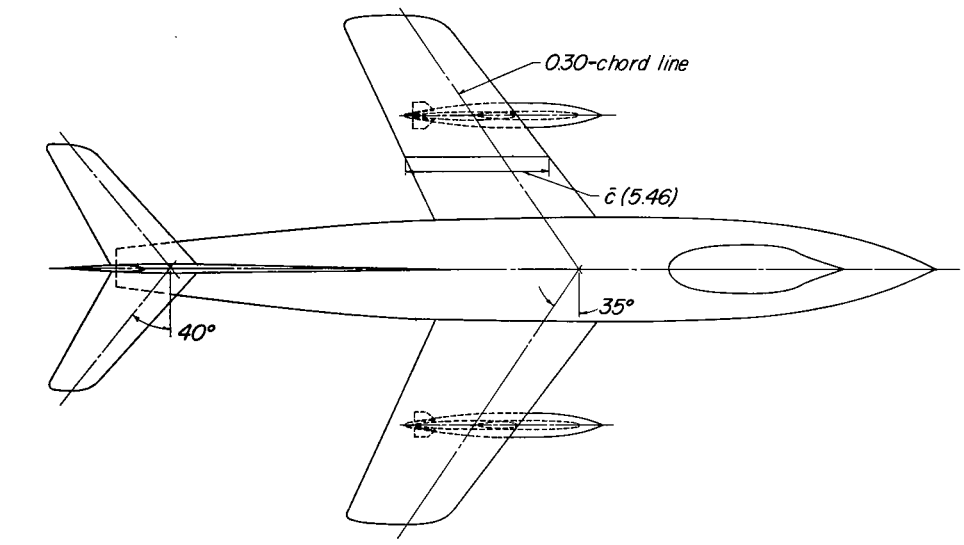

Wing Geometry

Airfoil sections (normal to 0.30-chord line)	
Root	*NACA 63-010*
Tip	*NACA 63-010*
Area, sq ft	*0.684*
Root chord, in.	*6.78*
Tip chord, in.	*3.83*
Aspect ratio	*3.57*
Taper ratio	*0.565*

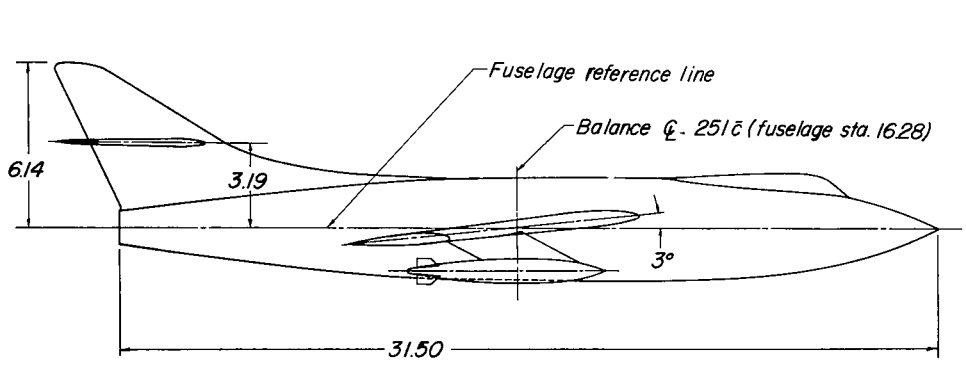

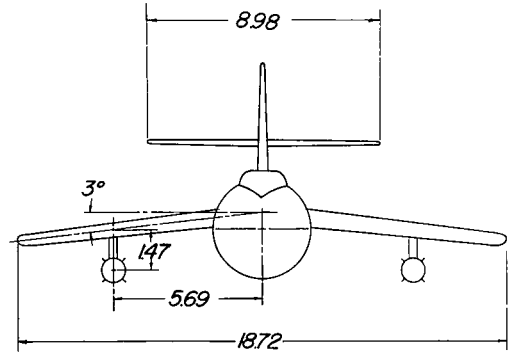

Figure 1.- Drawing of 1/16-scale model of the Douglas D-558-II research airplane. All dimensions are in inches.

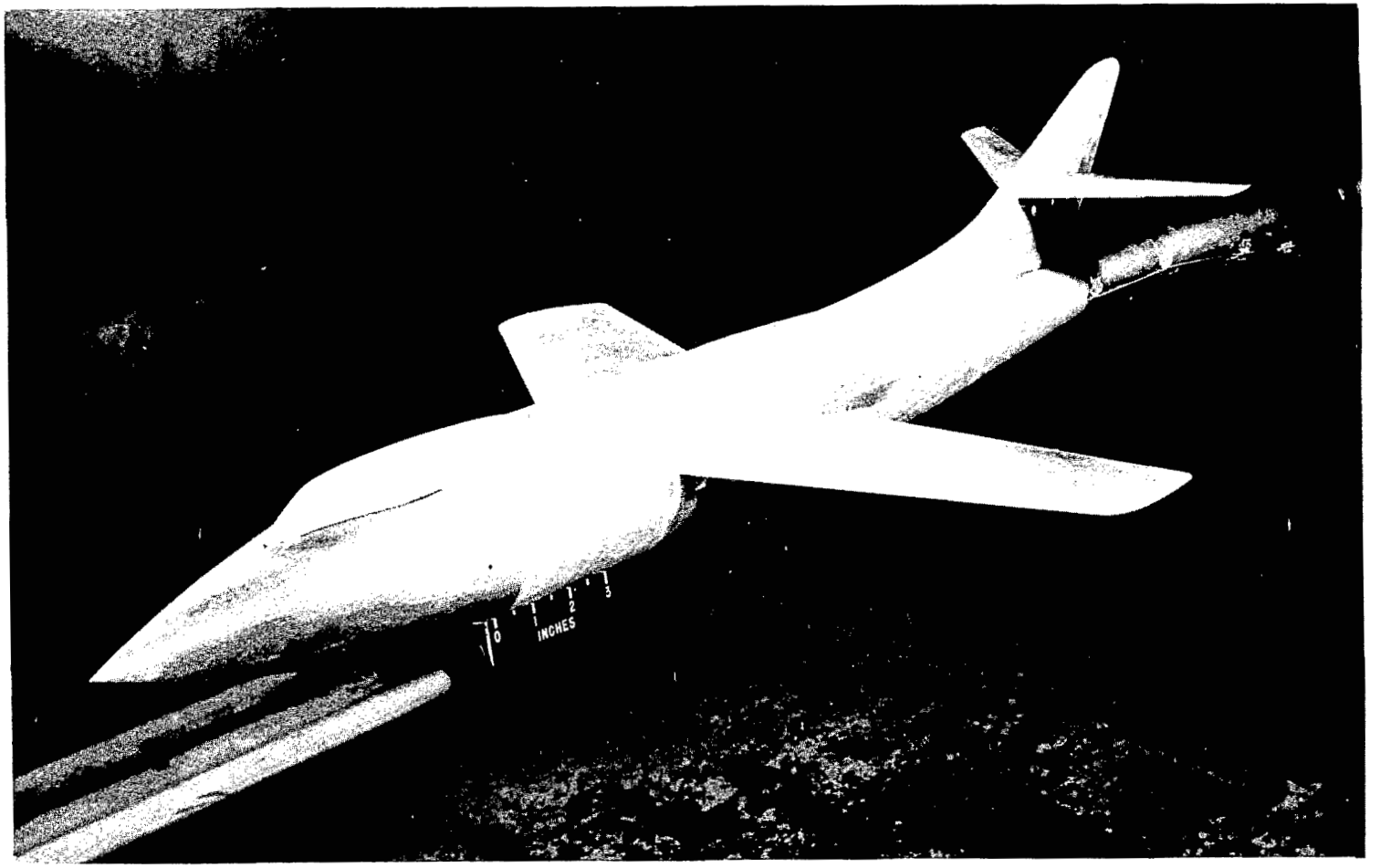

L-74746

(a) Model without stores.

Figure 2.- Photographs of a 1/16-scale model of the Douglas D-558-II research airplane in the Langley high-speed 7- by 10-foot tunnel.

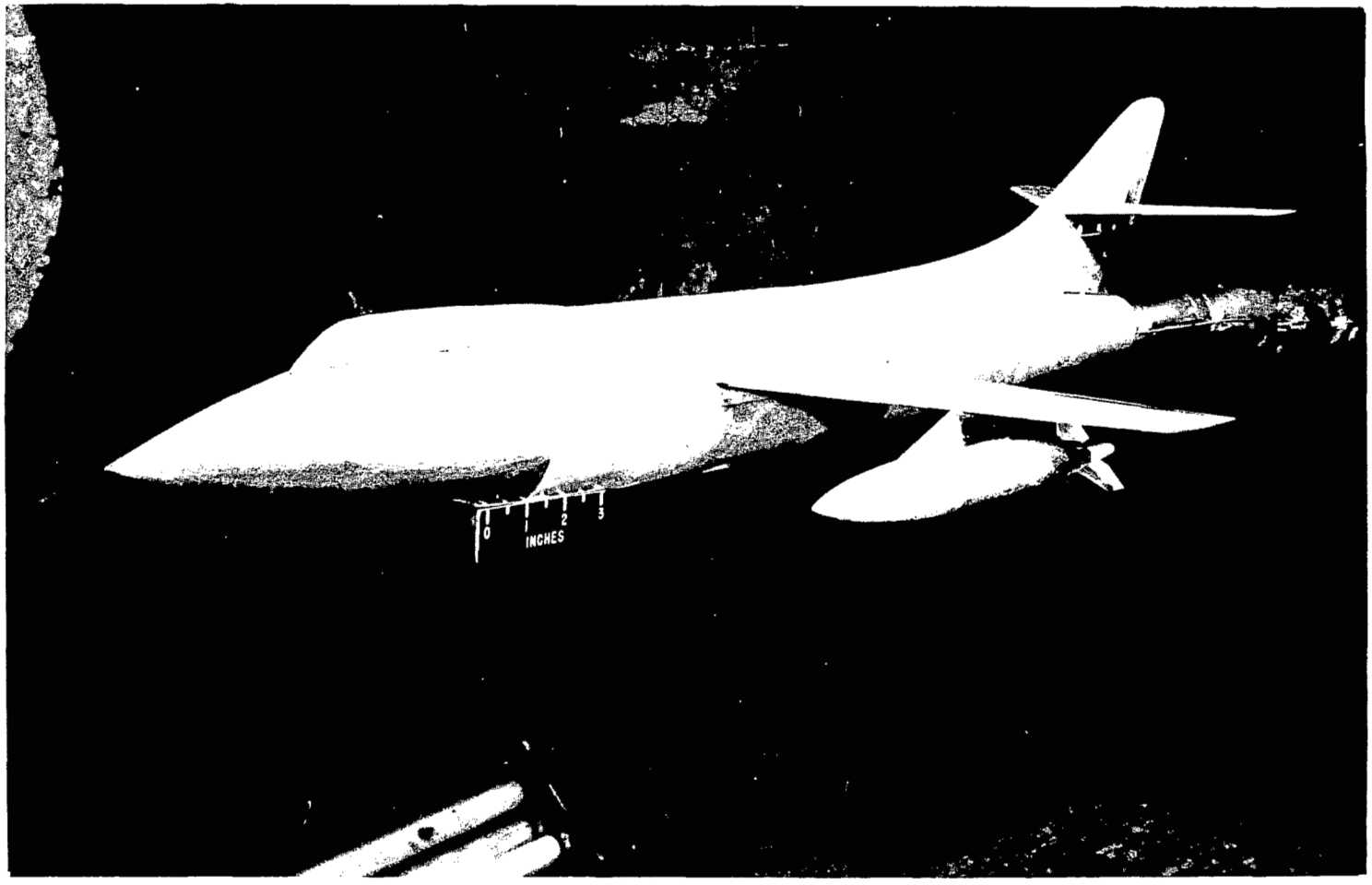

L-74749

(b) Model with stores B and 7.6-percent-thick pylons.

Figure 2.- Concluded.

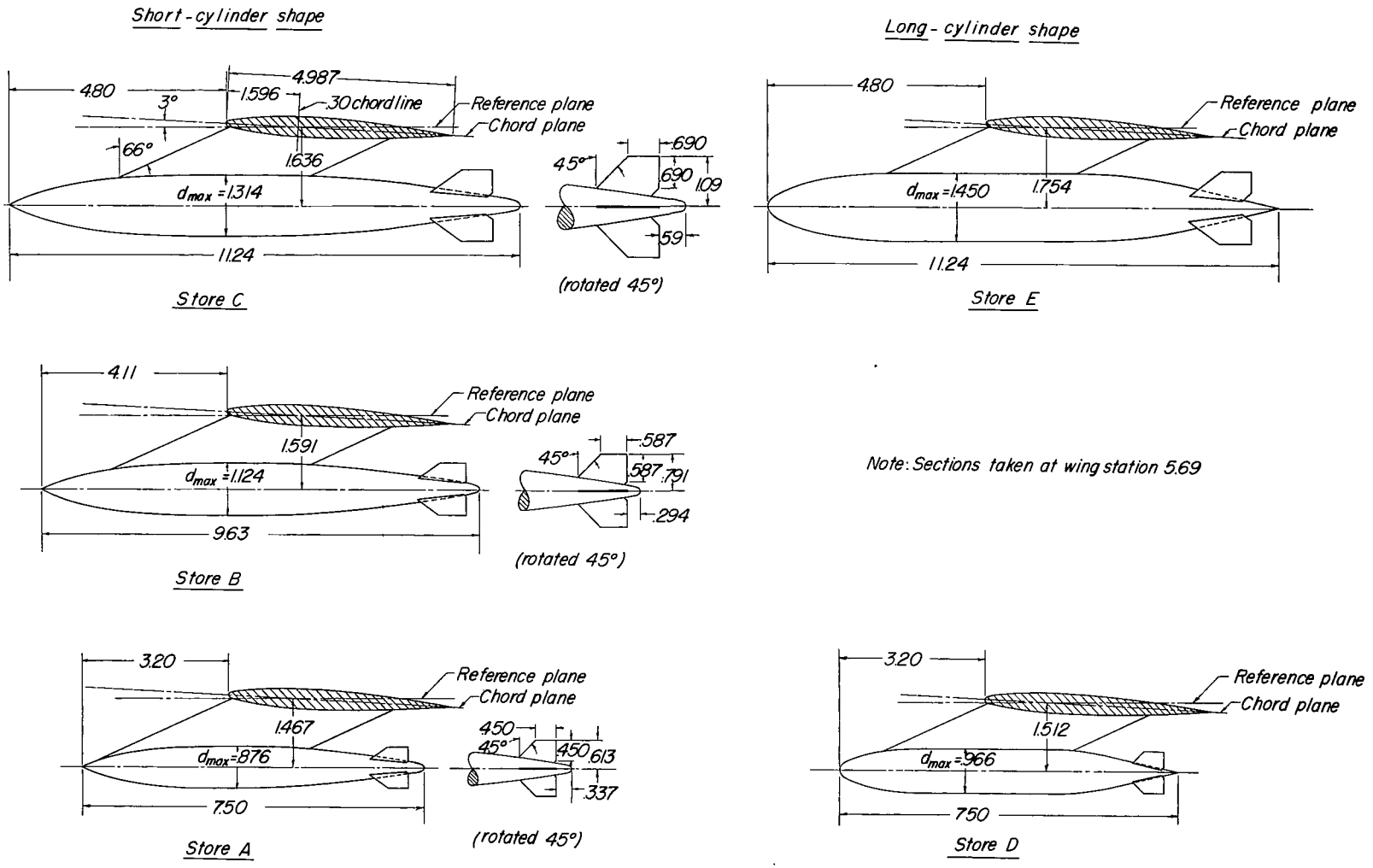

Figure 3.- Drawing of the stores tested on a 1/16-scale model of the Douglas D-558-II research airplane. All dimensions are in inches.

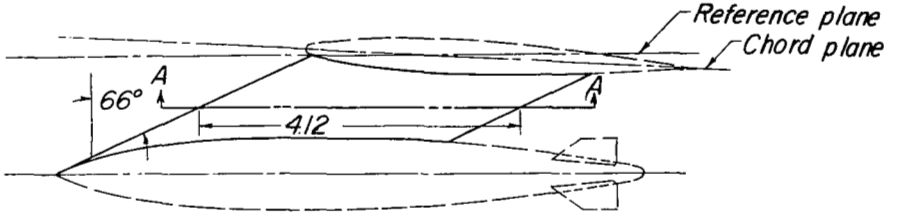

7.6 % thick pylon

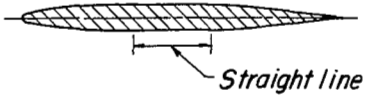

Section A - A

x	y	x	y
0	0	Straight line	
L.E.R	.017	2.41	.156
.031	.032	2.56	.155
.063	.045	2.72	.151
.156	.070	2.88	.144
.313	.096	3.03	.134
.468	.114	3.19	.121
.625	.128	3.34	.105
.782	.138	3.66	.066
.938	.146	3.97	.021
1.195	.152	4.12	0
1.250	.156		
1.407	.156		

6.2 % thick pylon

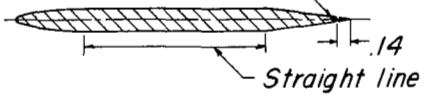

Section A-A

x	y
0	0
.200	.082
.400	.108
.600	.122
.852	.128
Straight line	
3.195	.128
4.260	0
4.120	T.E.R. =.019

4.2 % thick pylon

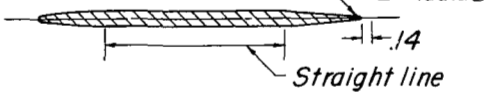

Section A-A

x	y
0	0
.200	.058
.400	.076
.600	.086
.852	.090
Straight line	
3.195	.090
4.260	0
4.120	T.E.R. =.013

Figure 4.- Drawing of the pylons tested on a 1/16-scale model of the Douglas D-558-II airplane. All dimensions are in inches. Dimensions given parallel to free stream.

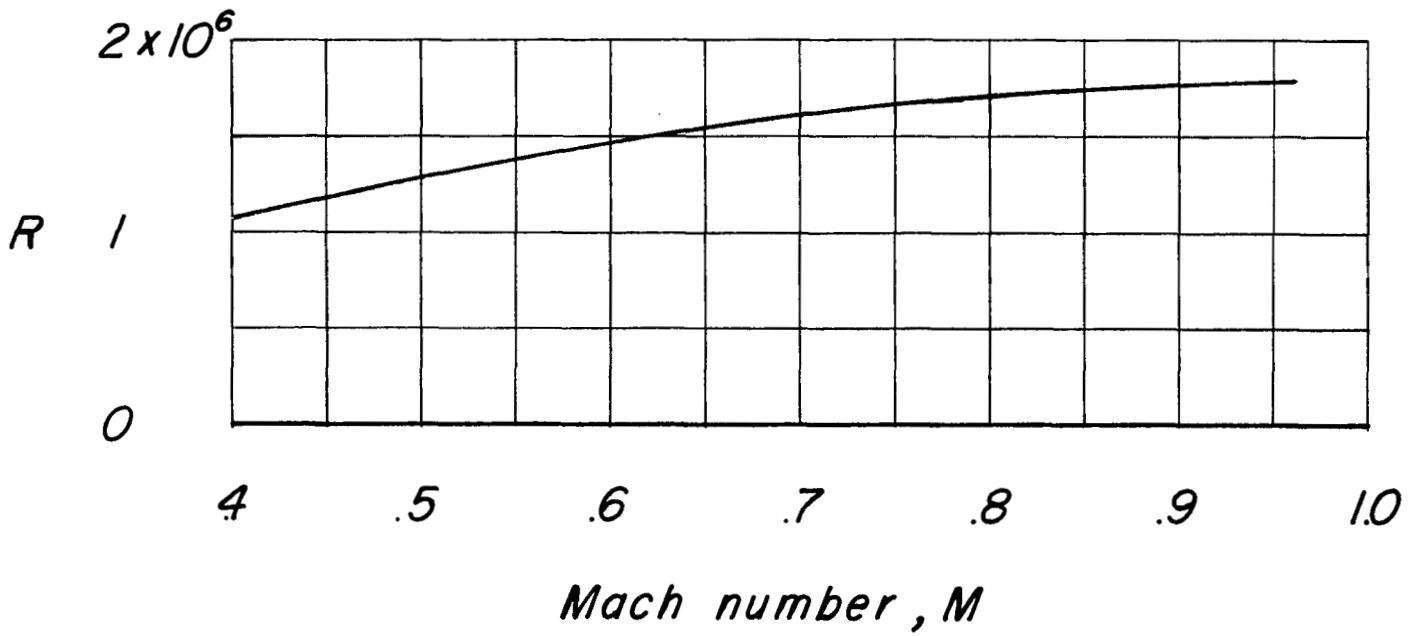

Figure 5.- Variation of Reynolds number with Mach number.

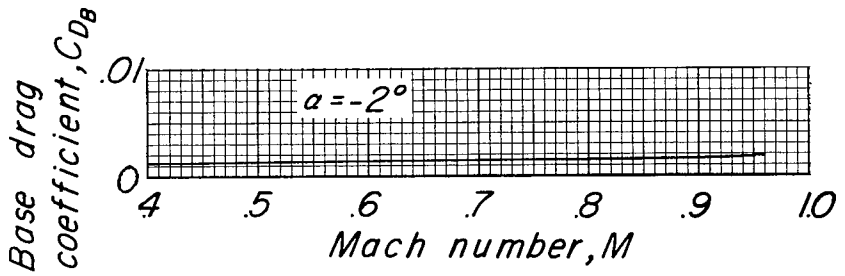

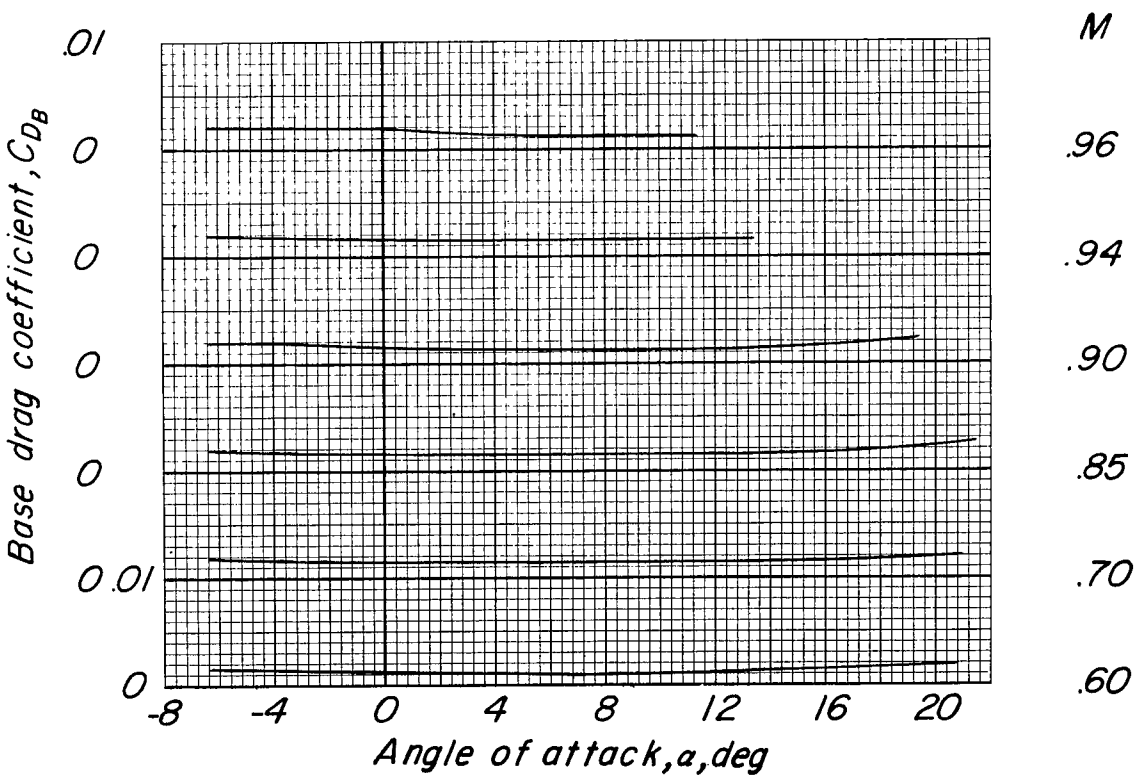

Figure 6.- Base drag coefficient of a 1/16-scale model of the Douglas D-558-II airplane with and without external stores.

[redacted]

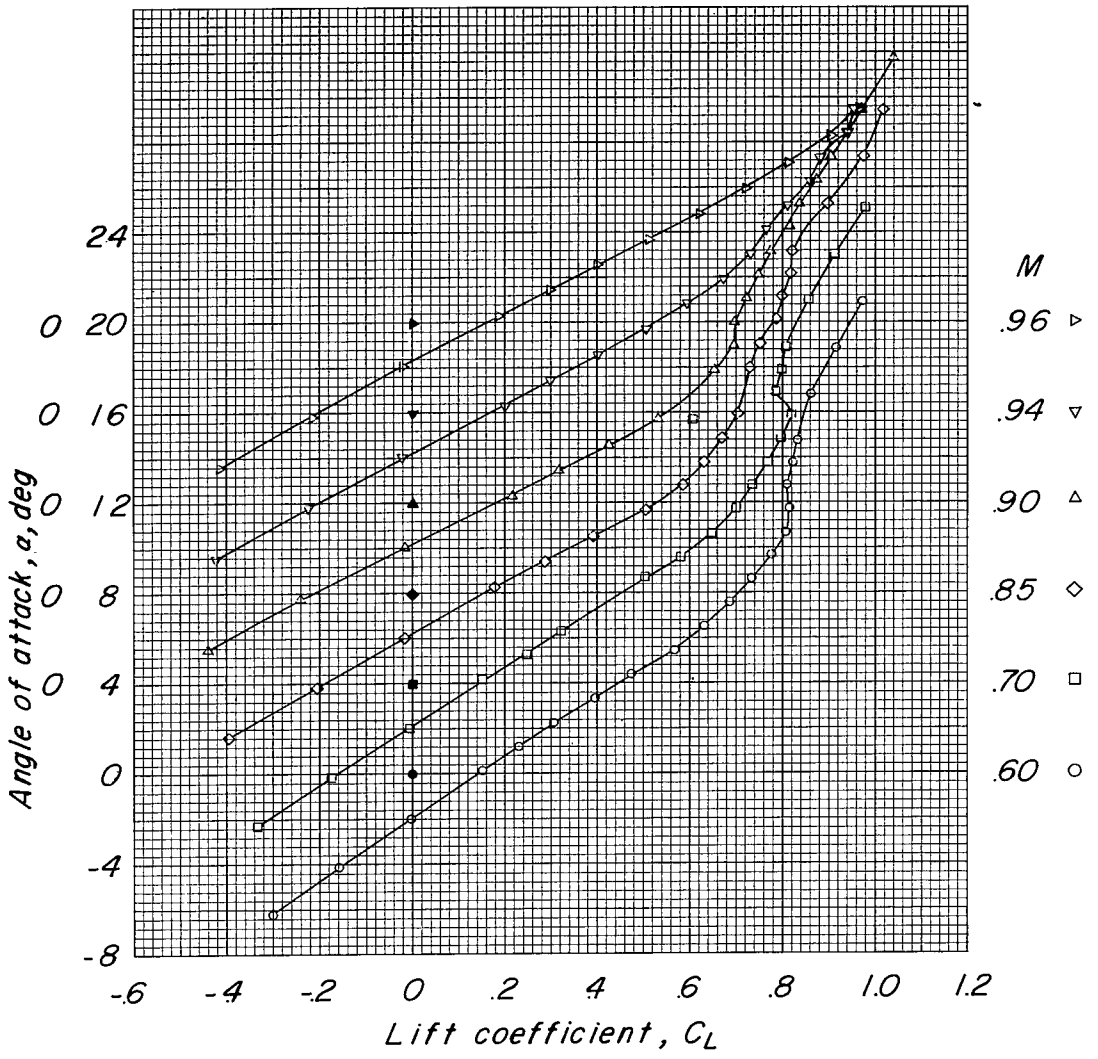

(a) α against C_L.

Figure 7.- Aerodynamic characteristics of a 1/16-scale model of the Douglas D-558-II airplane. $i_t = 0^\circ$.

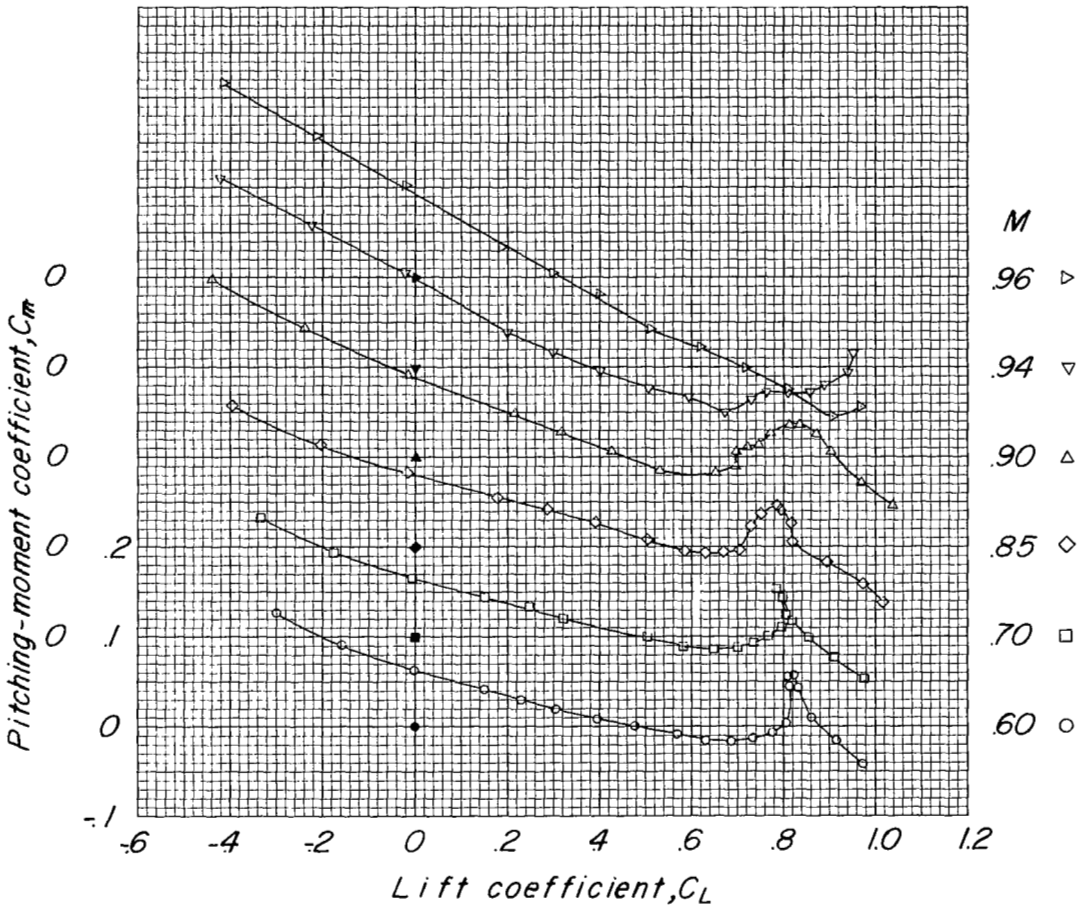

(b) C_m against C_L.

Figure 7.- Continued.

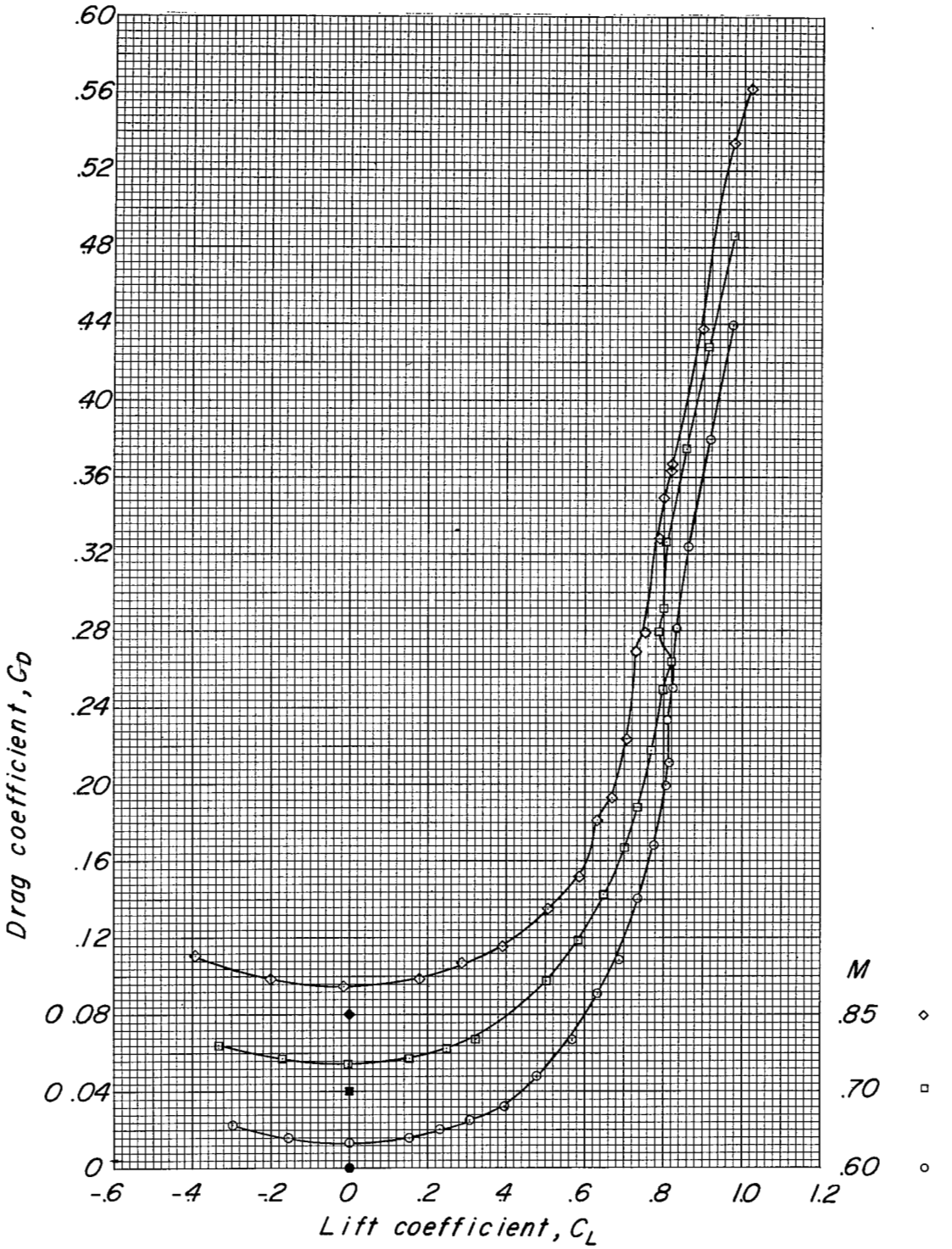

(c) C_D against C_L.

Figure 7.- Continued.

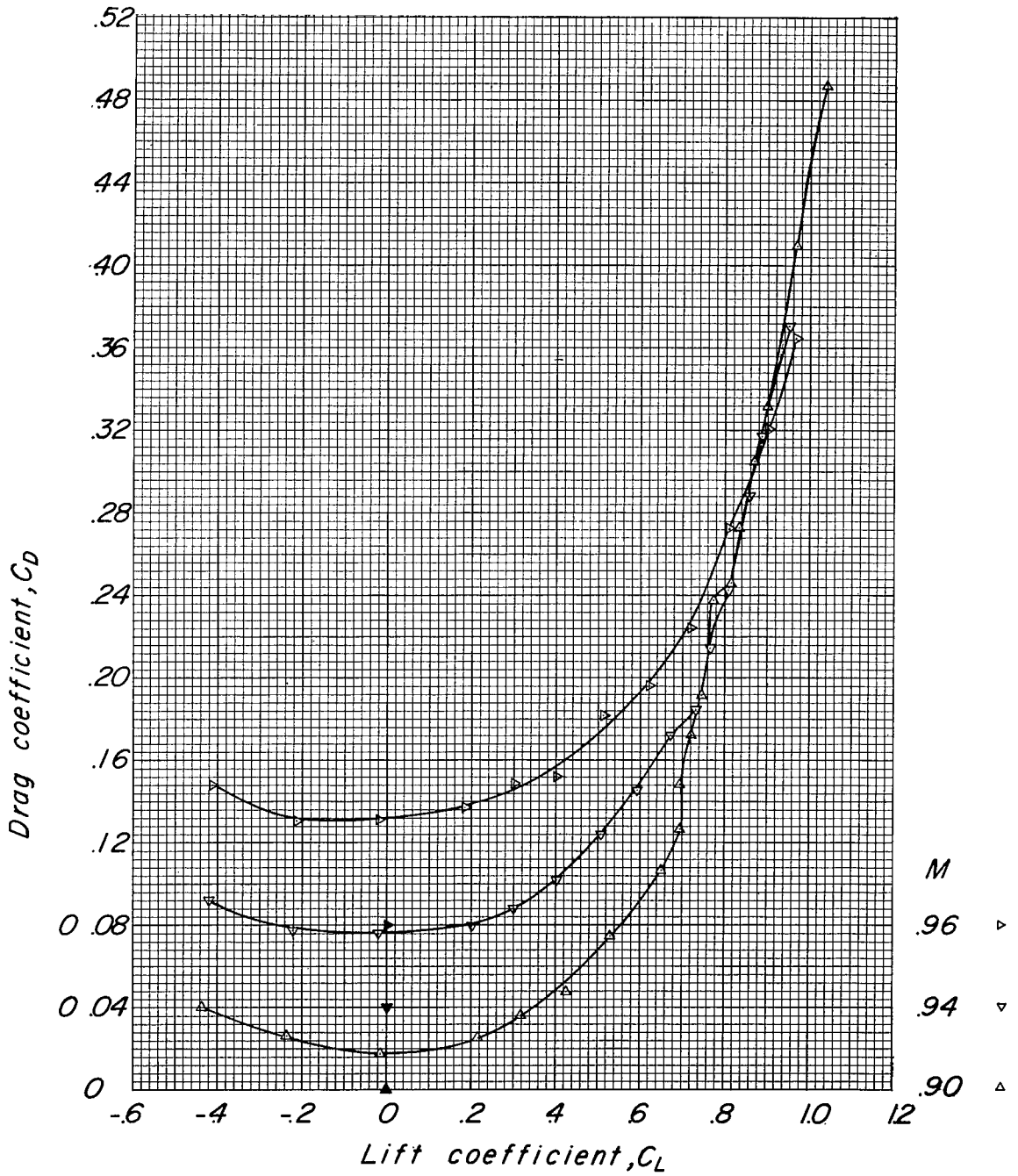

(c) Concluded.

Figure 7.- Concluded.

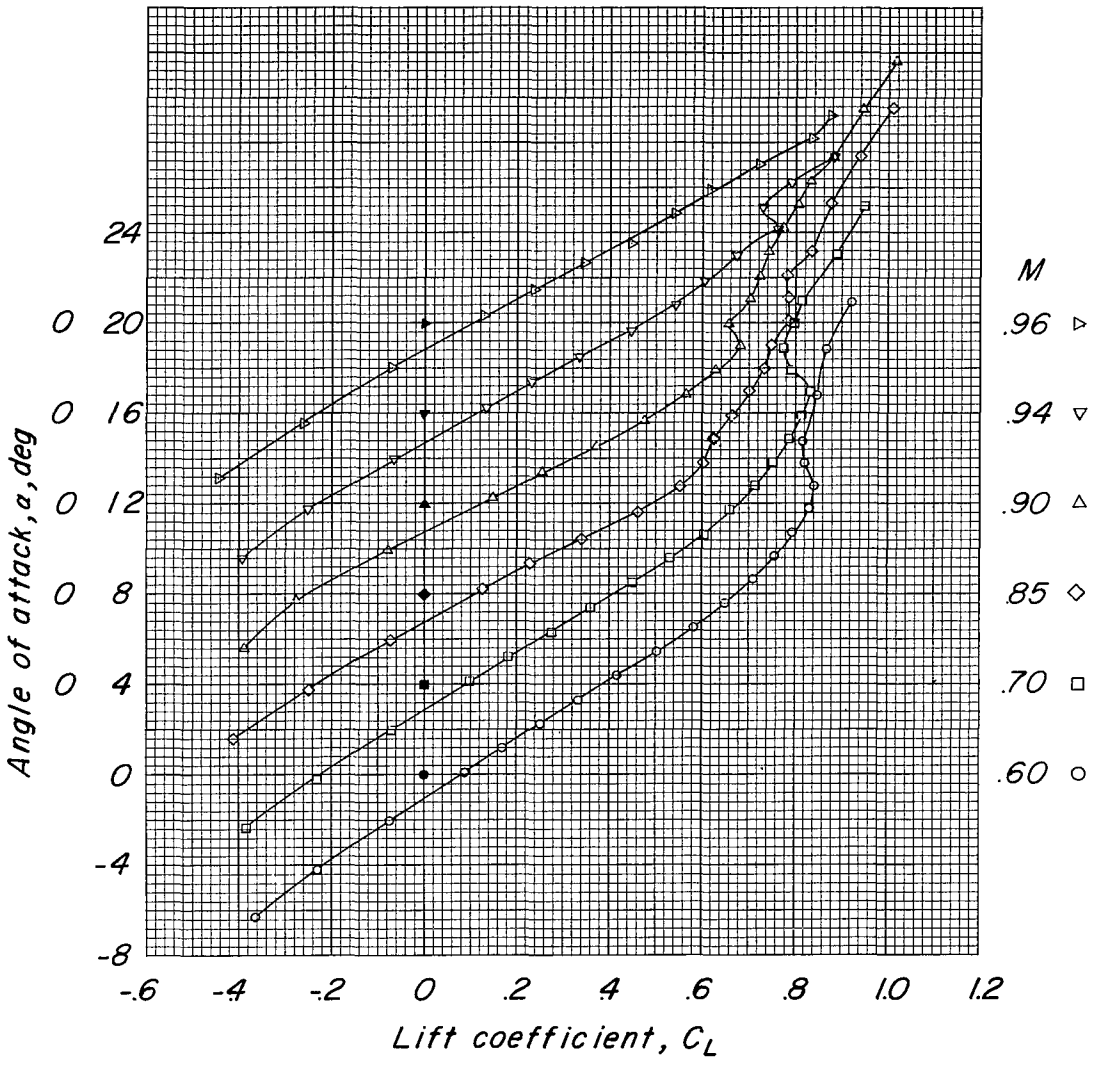

(a) α against C_L.

Figure 8.- Aerodynamic characteristics of a 1/16-scale model of the Douglas D-558-II airplane with stores A plus 7.6-percent pylons. $i_t = 0^\circ$.

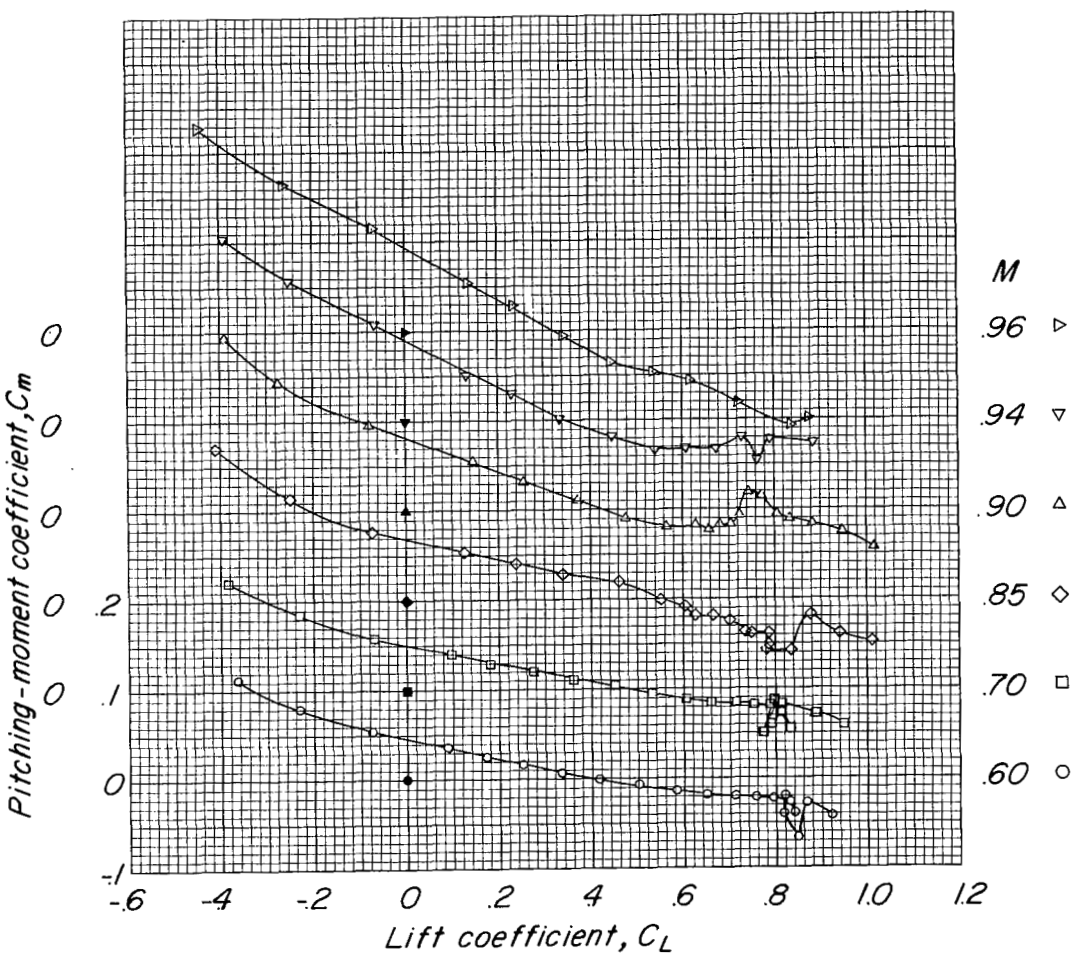

(b) C_m against C_L.

Figure 8.- Continued.

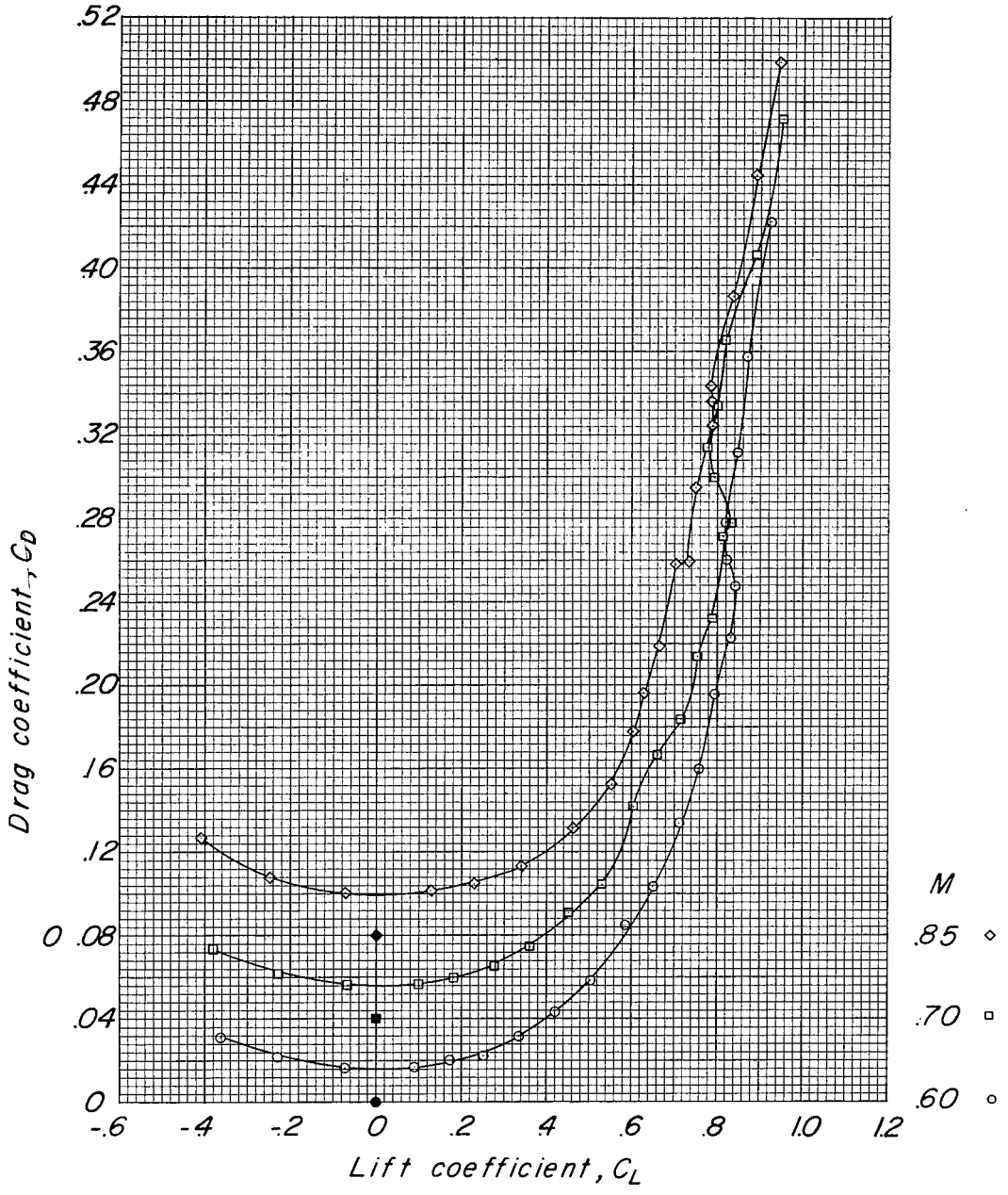

(c) C_D against C_L.

Figure 8.- Continued.

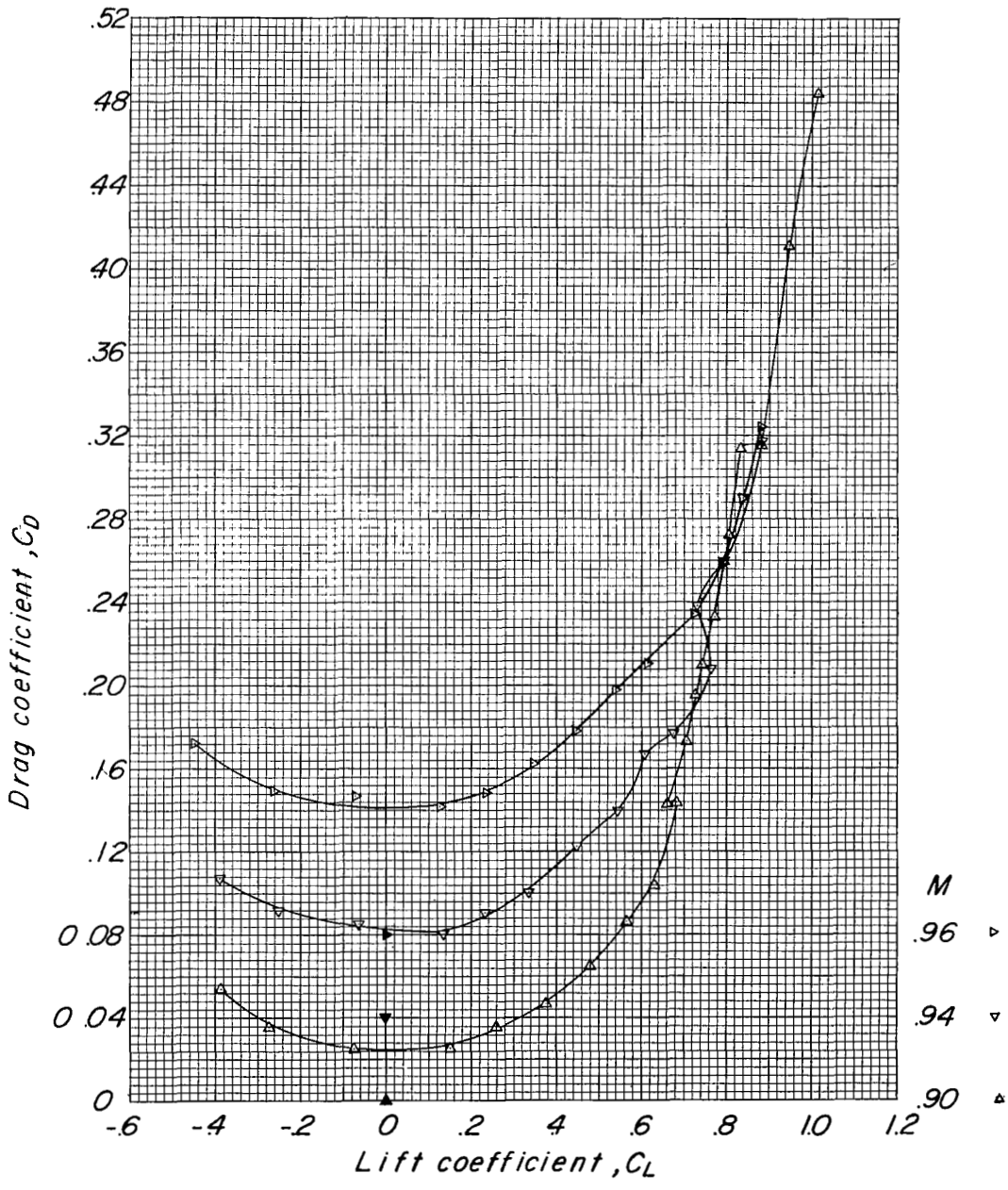

(c) Concluded.

Figure 8.- Concluded.

[redacted]

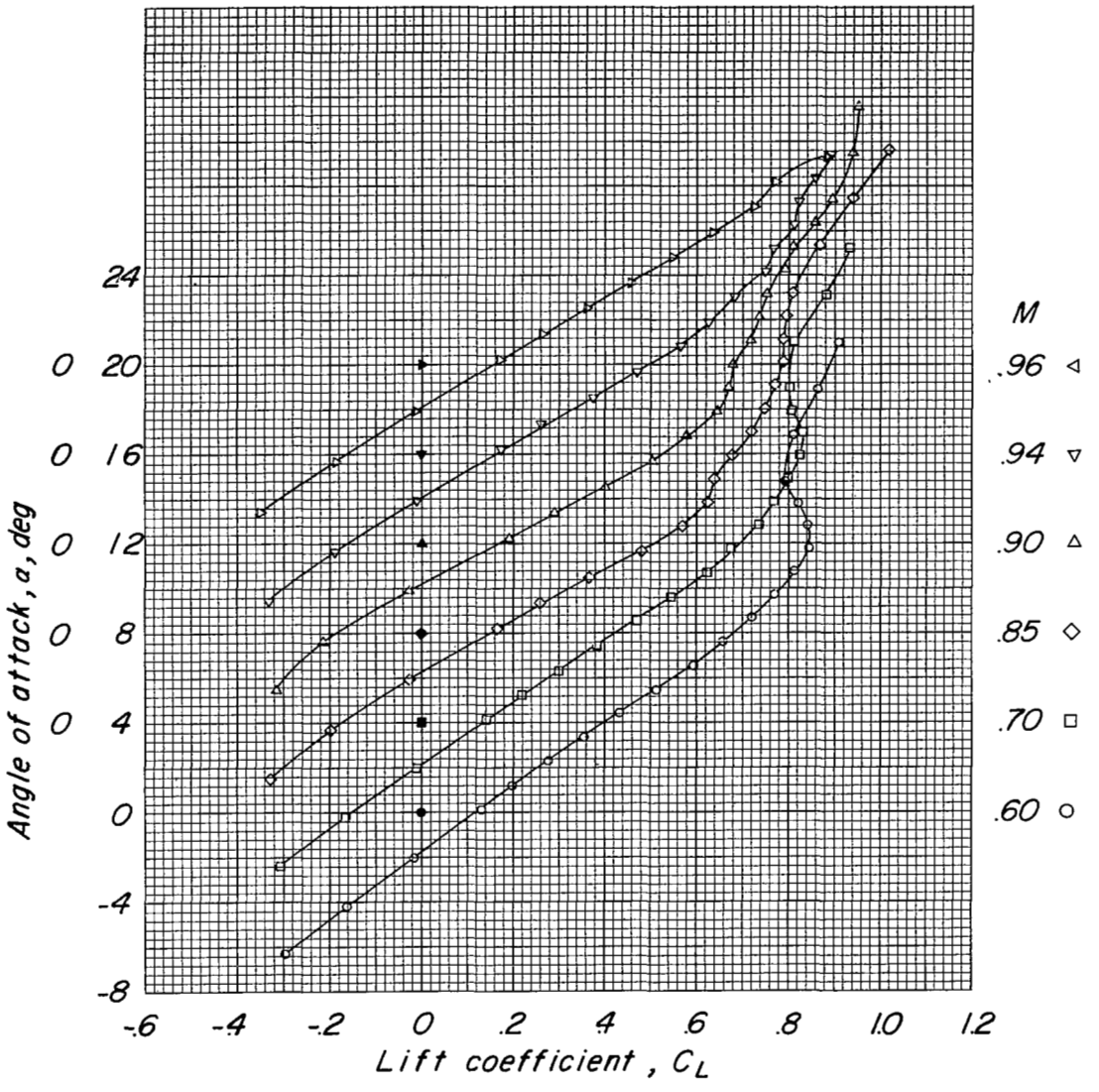

(a) α against C_L.

Figure 9.- Aerodynamic characteristics of a 1/16-scale model of the Douglas D-558-II airplane with stores A plus 7.6-percent pylons. Horizontal tail off.

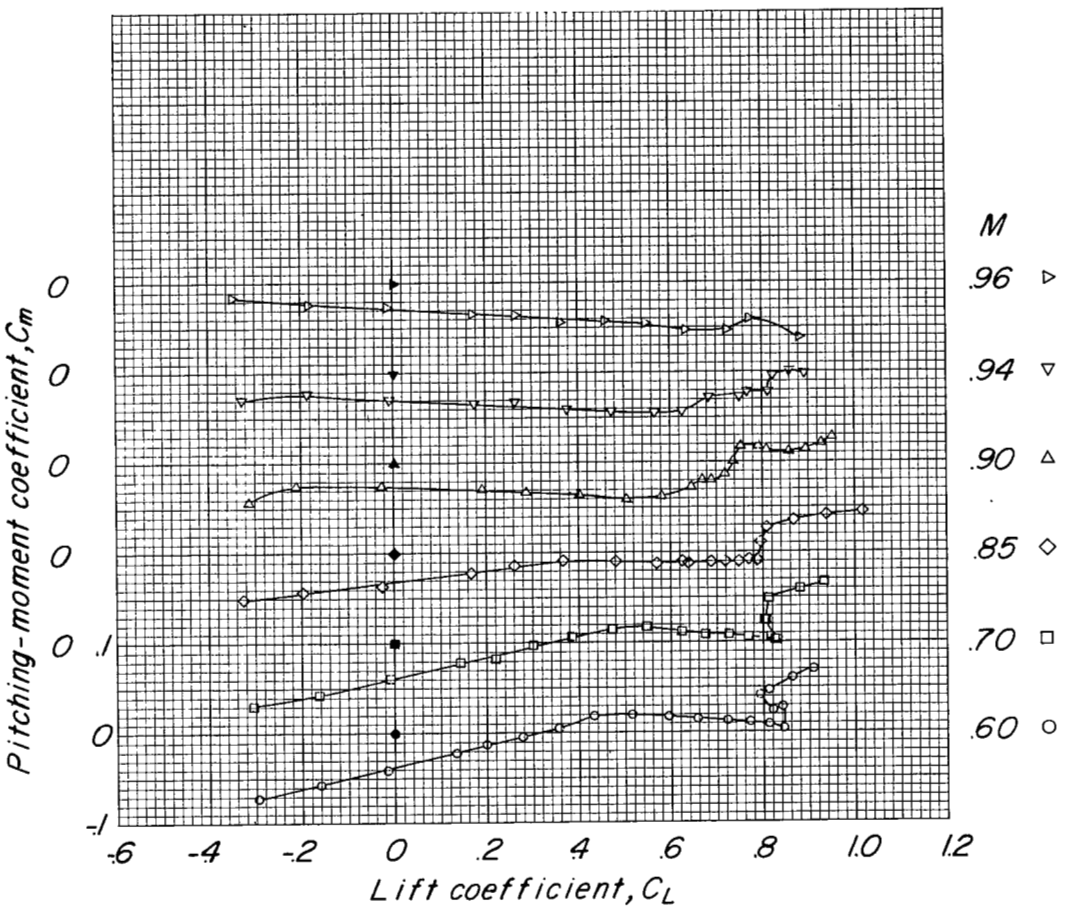

(b) C_m against C_L.

Figure 9.- Continued.

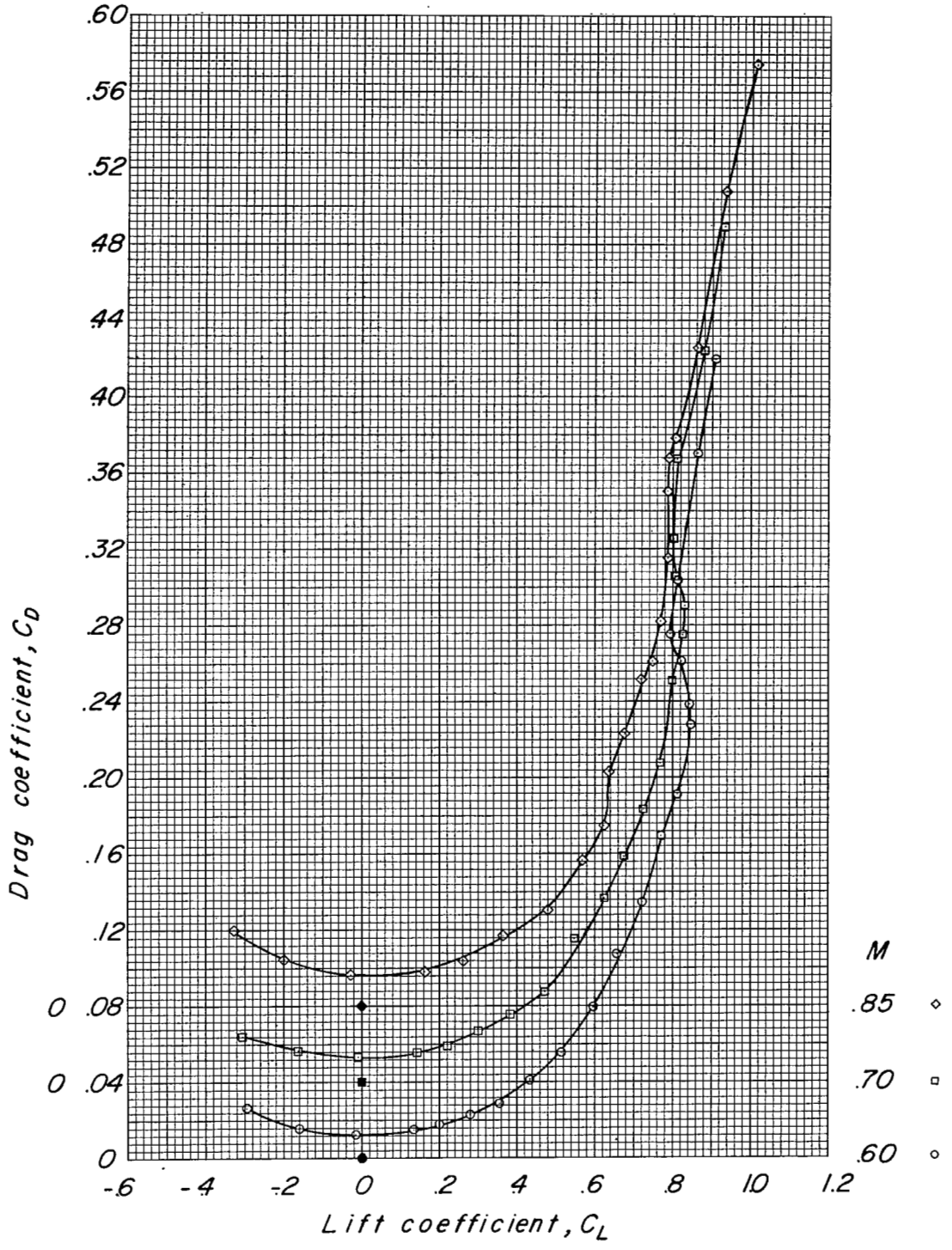

(c) C_D against C_L.

Figure 9.- Continued.

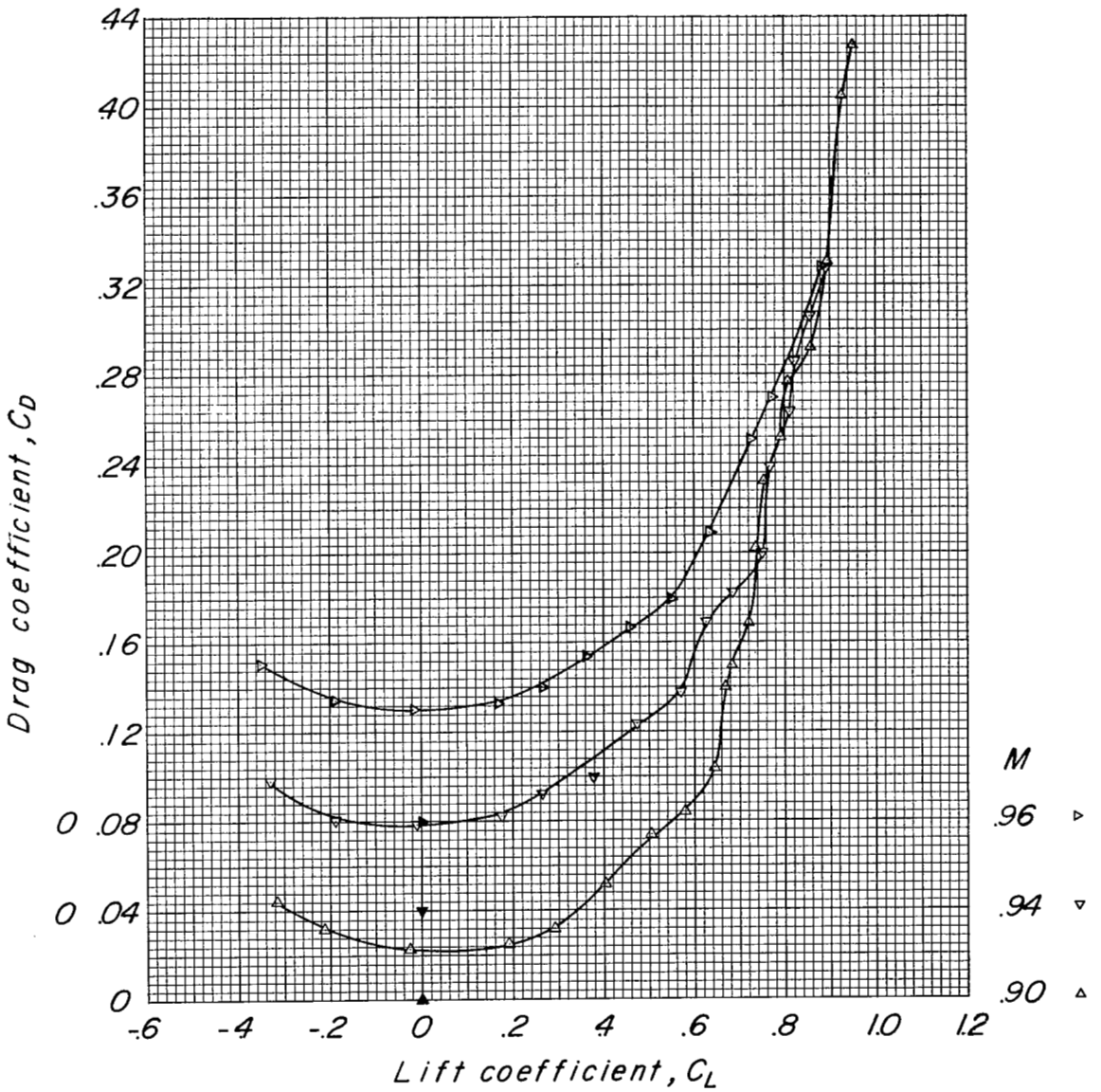

(c) Concluded.

Figure 9.- Concluded.

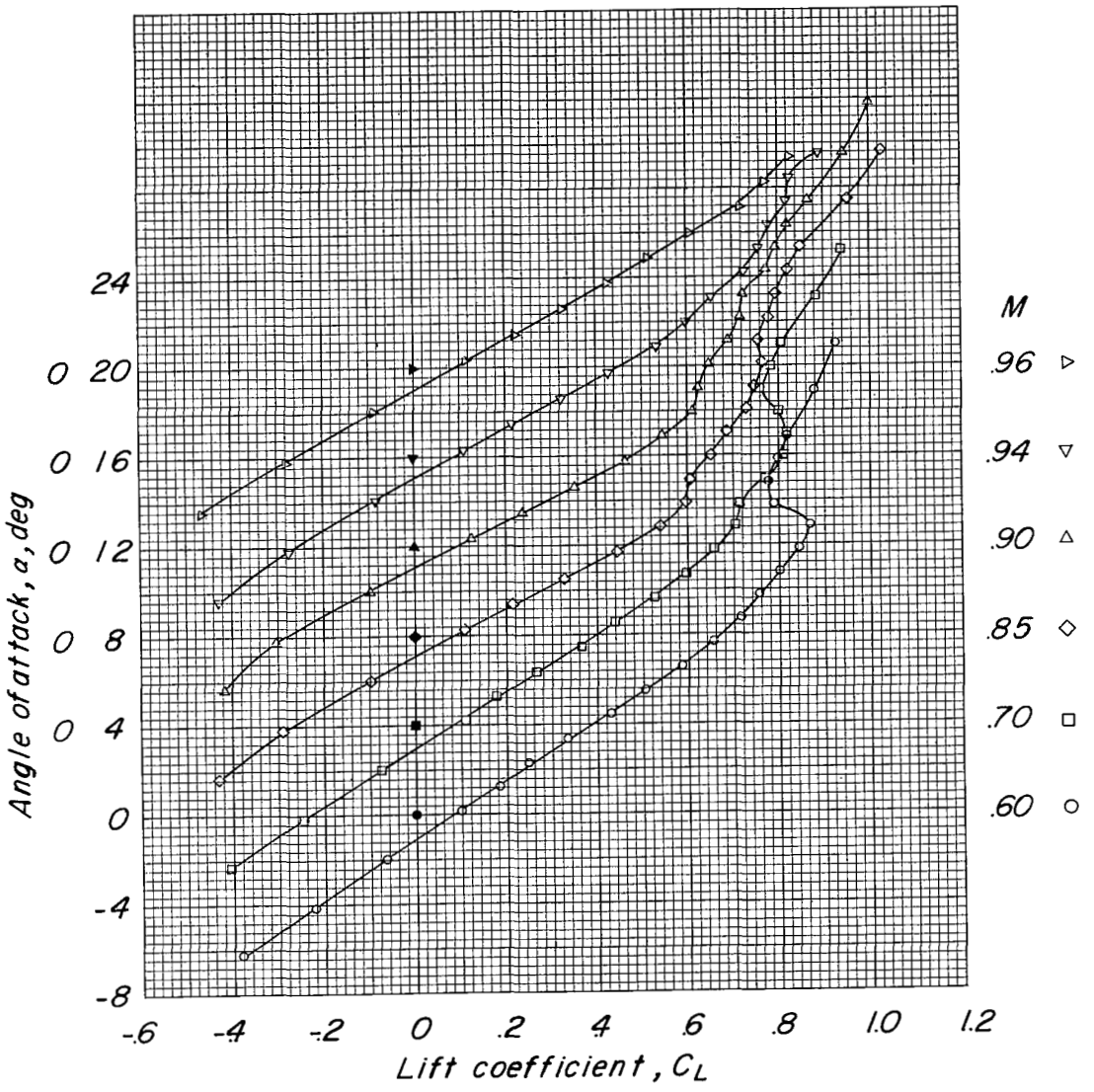

(a) α against C_L.

Figure 10.- Aerodynamic characteristics of a 1/16-scale model of the Douglas D-558-II airplane with stores A plus 7.6-percent pylons. $i_t = -2^\circ$.

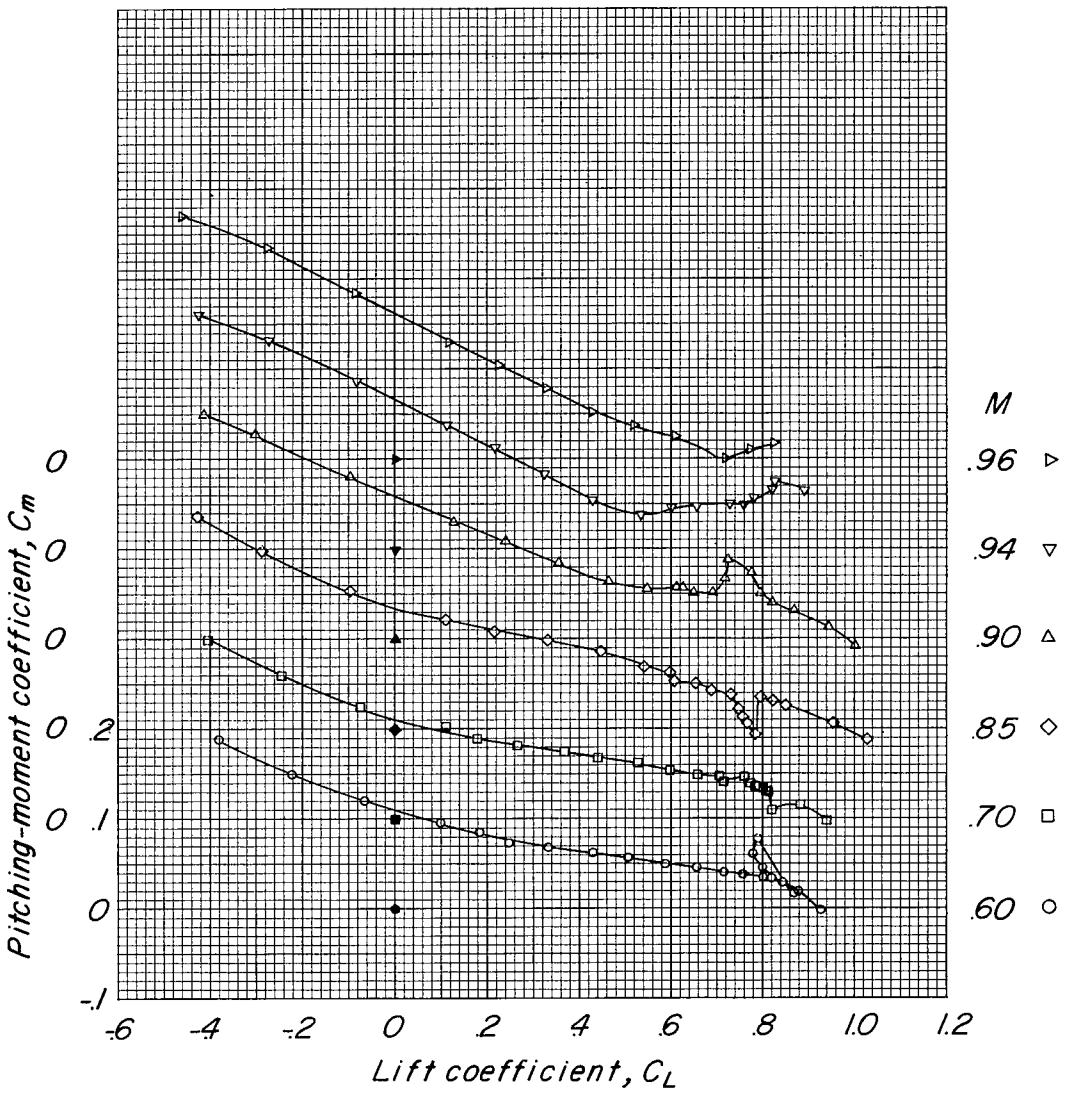

(b) C_m against C_L.

Figure 10.- Continued.

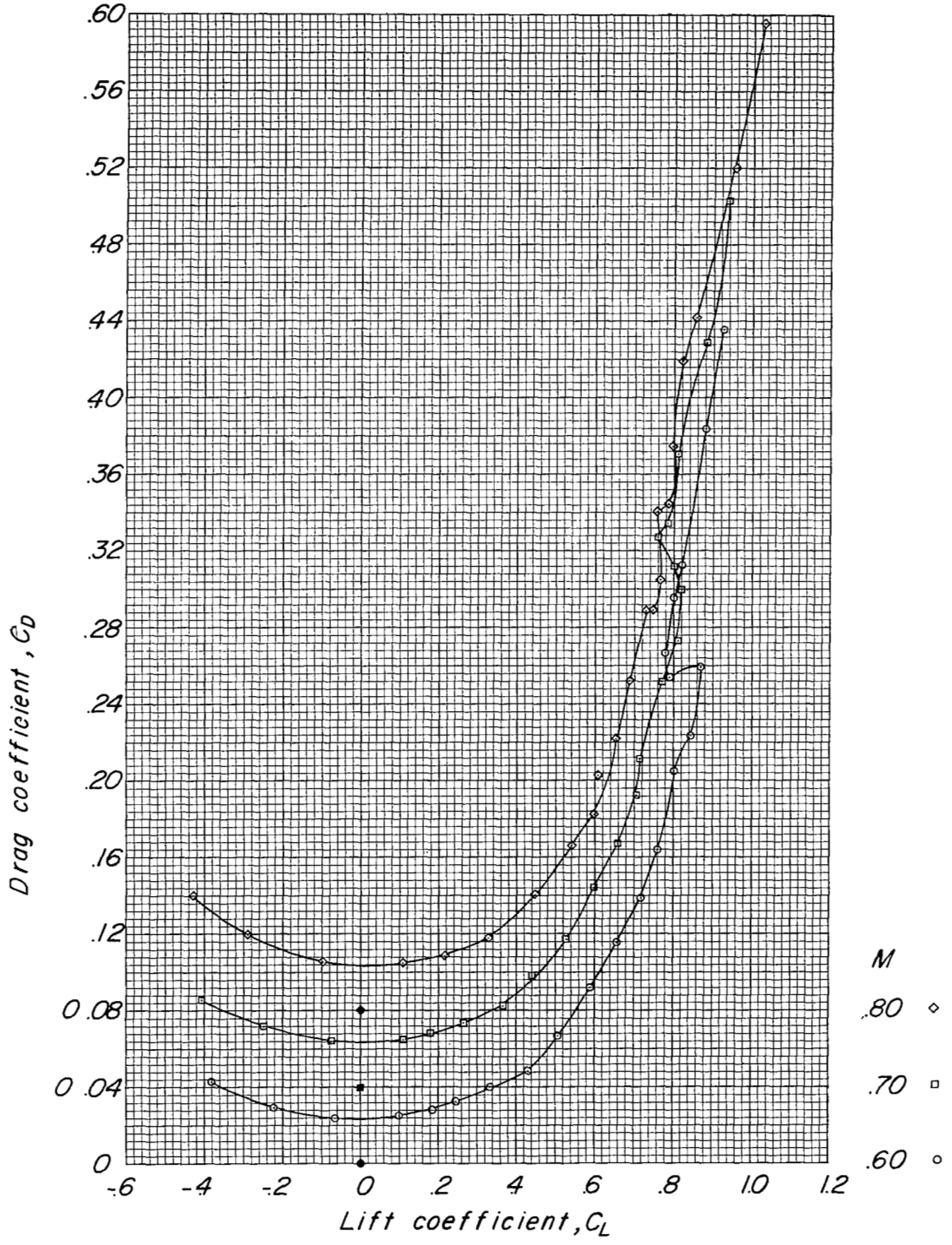

(c) C_D against C_L.

Figure 10.- Continued.

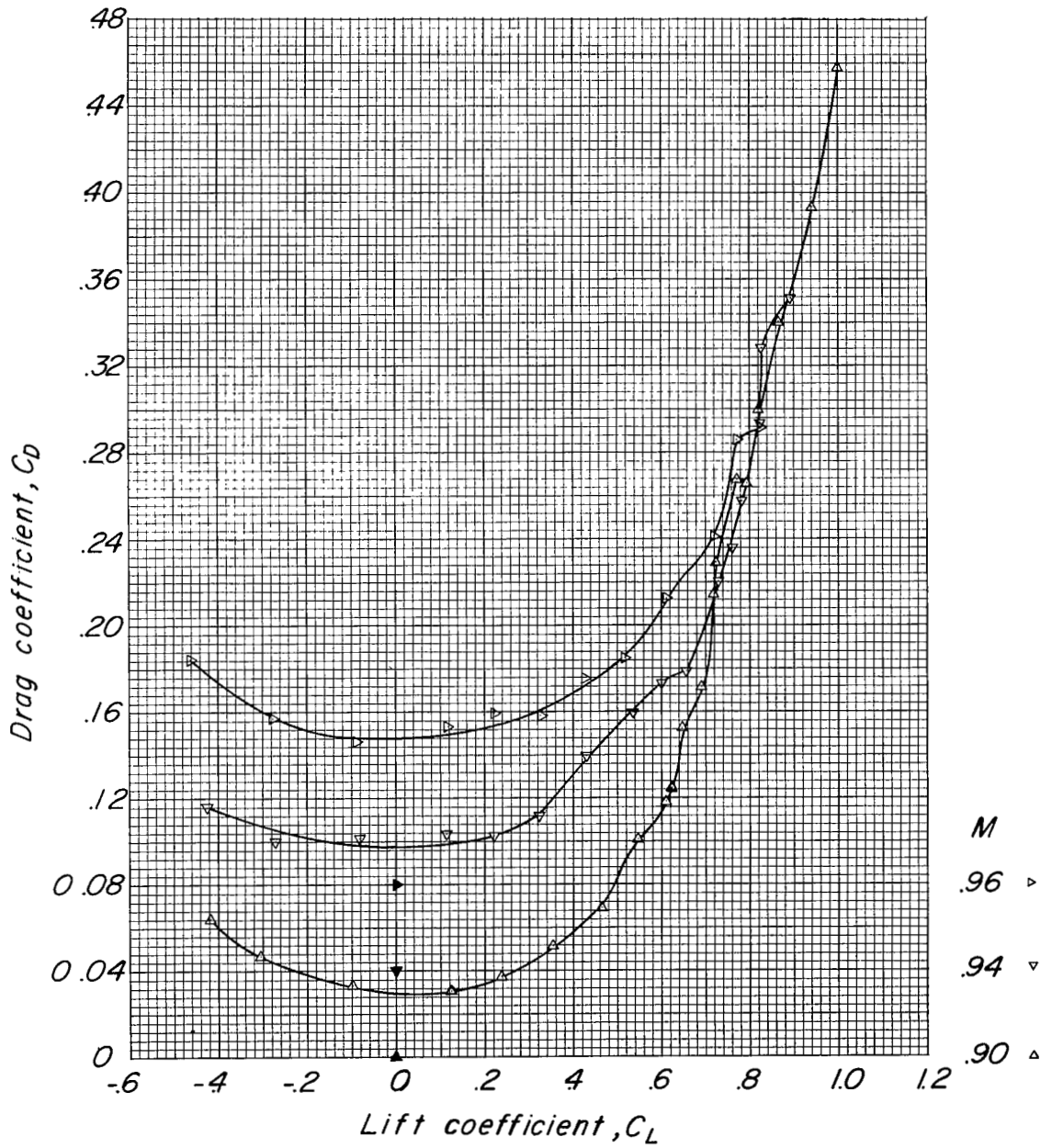

(c) Concluded.

Figure 10.- Concluded.

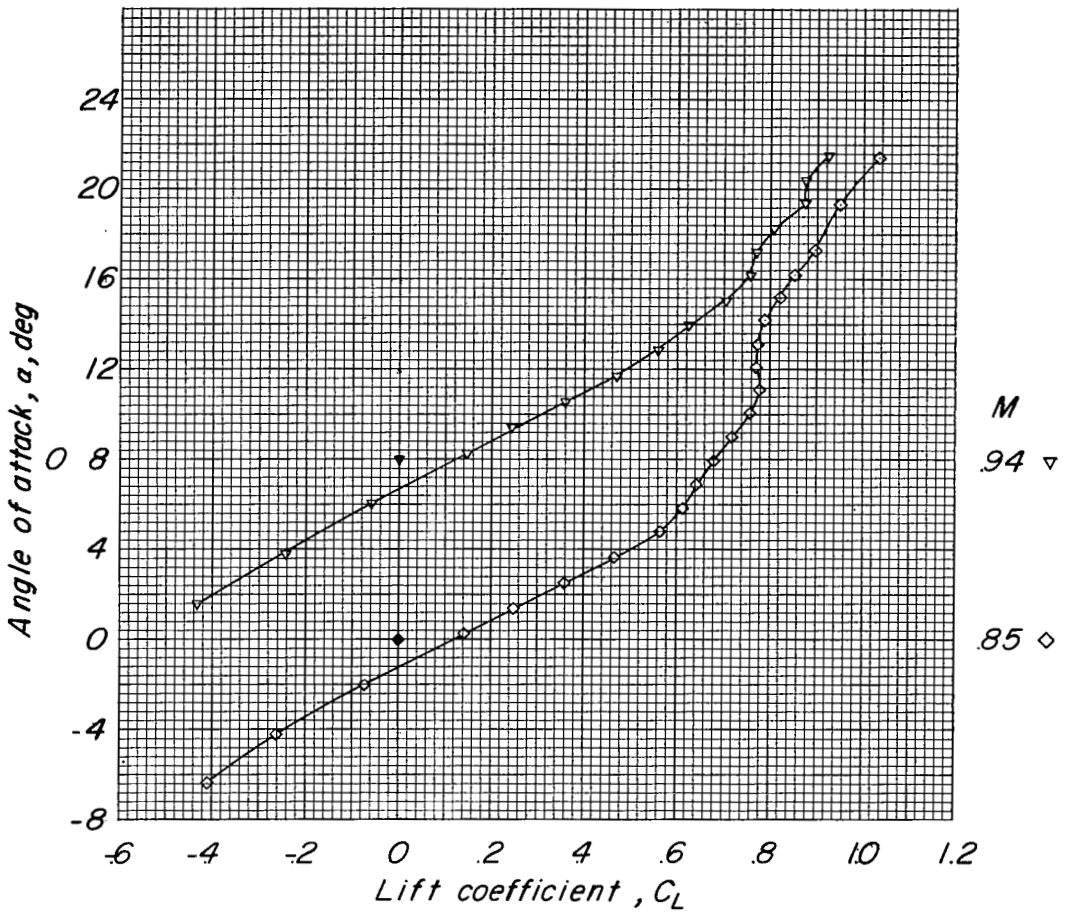

(a) α against C_L.

Figure 11.- Aerodynamic characteristics of a 1/16-scale model of the Douglas D-558-II airplane with stores A plus 6.2-percent pylons. $i_t = 0^\circ$.

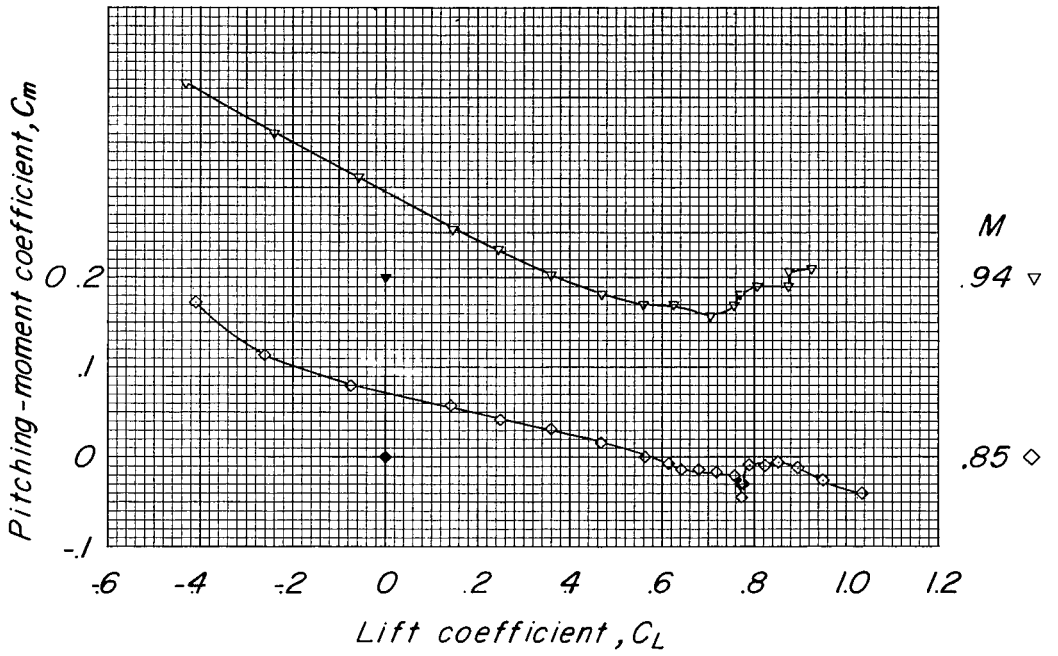

(b) C_m against C_L.

Figure 11.- Continued.

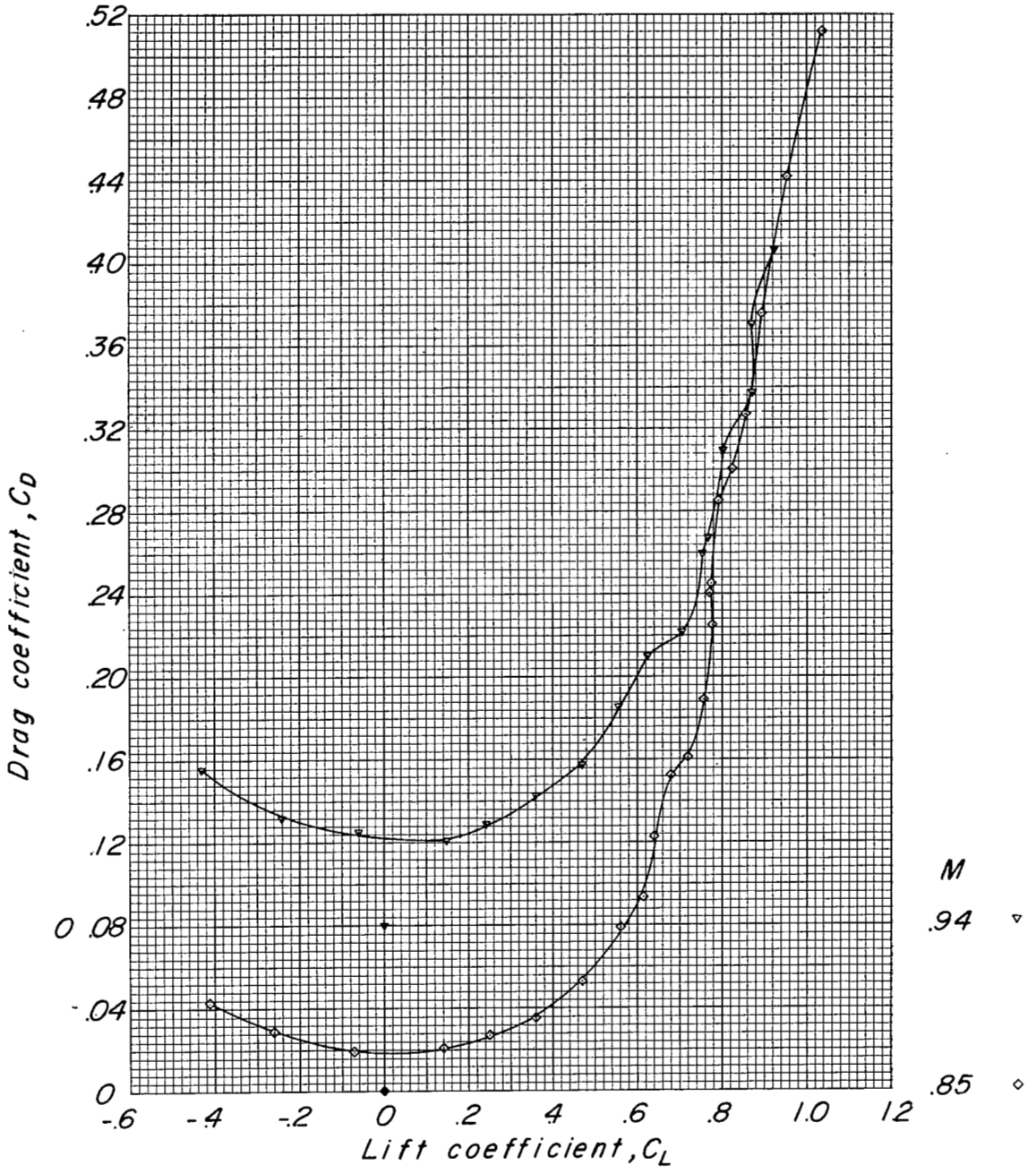

(c) C_D against C_L.

Figure 11.- Concluded.

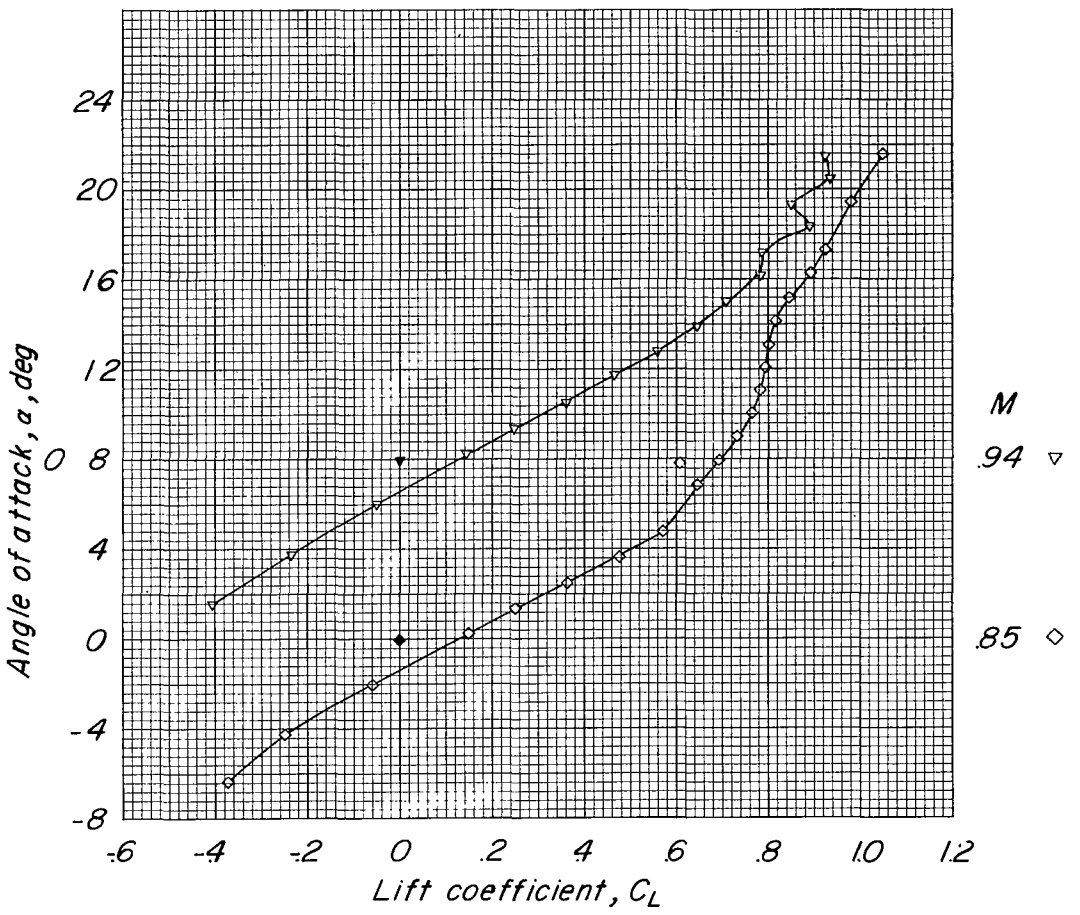

(a) α against C_L.

Figure 12.- Aerodynamic characteristics of a 1/16-scale model of the Douglas D-558-II airplane with stores A plus 4.2-percent pylons. $i_t = 0^\circ$.

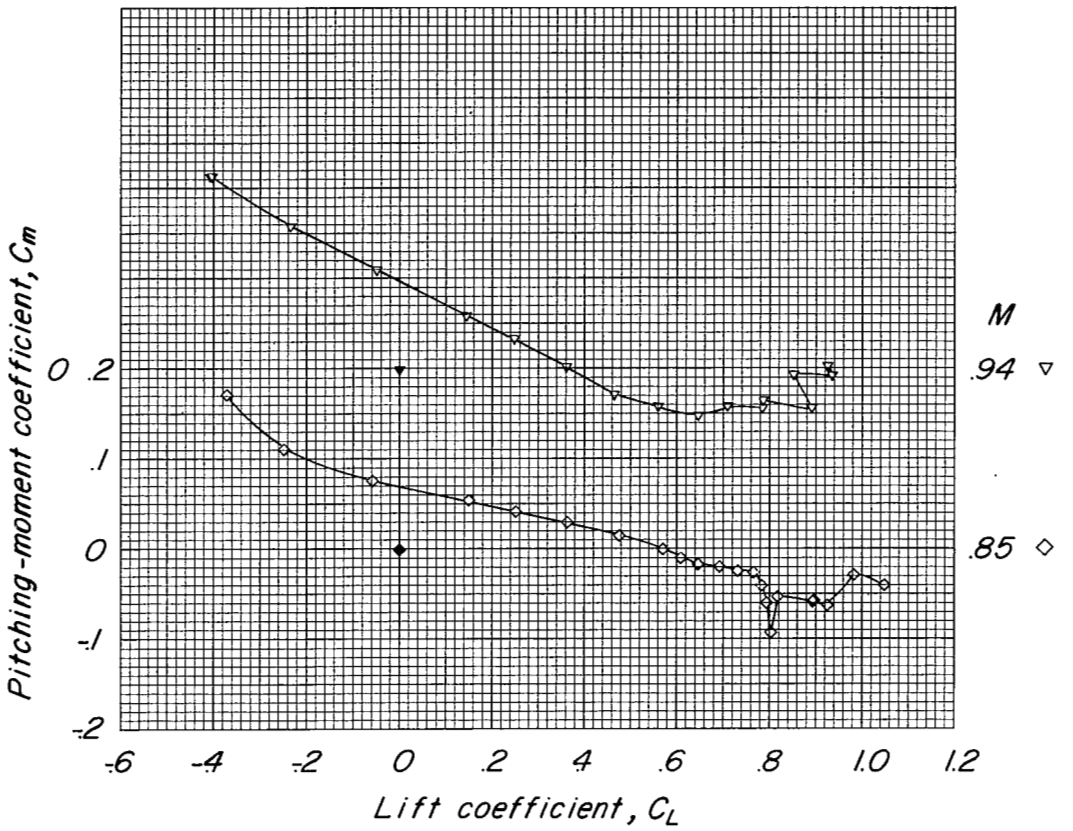

(b) C_m against C_L.

Figure 12.- Continued.

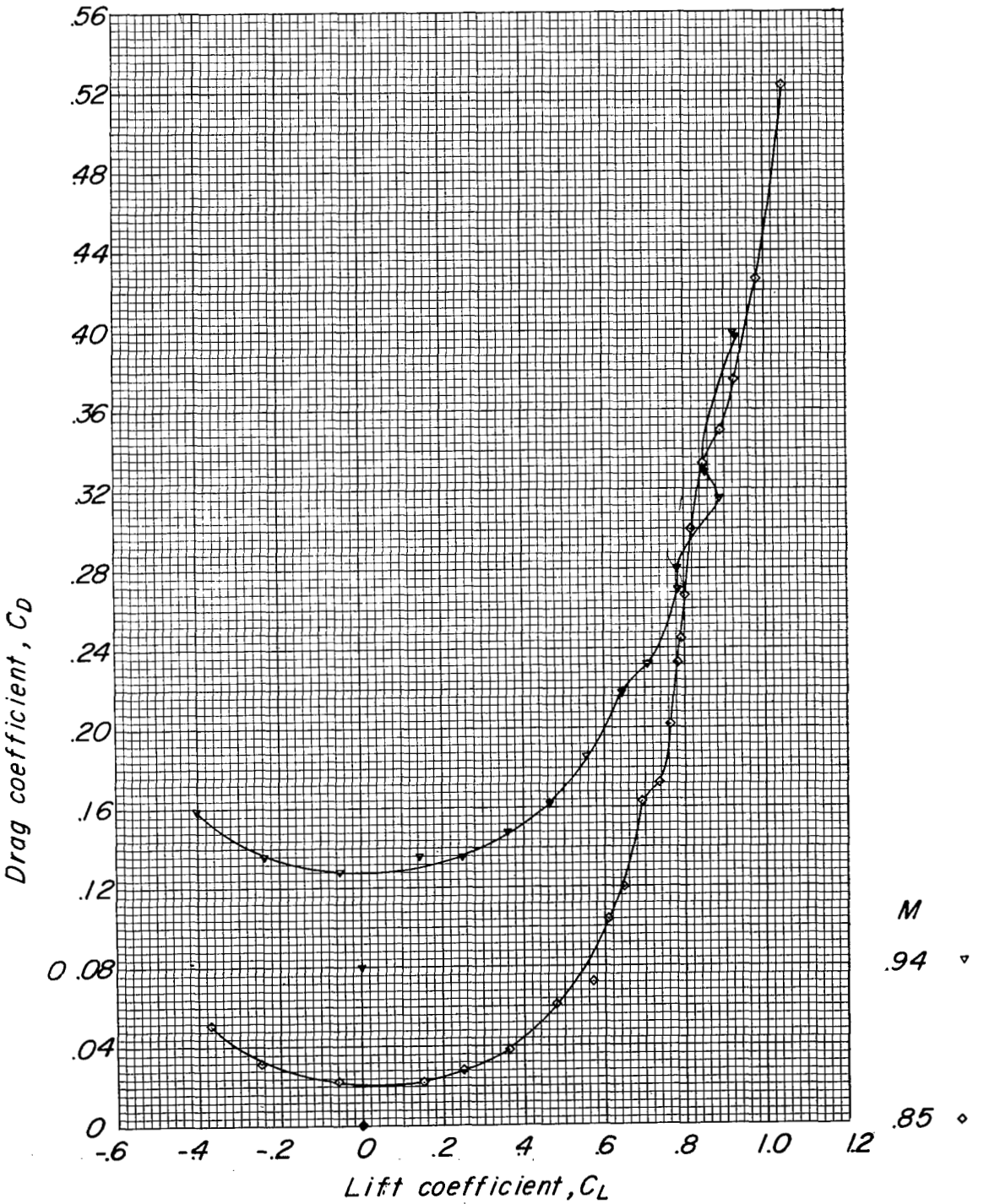

(c) C_D against C_L.

Figure 12.- Concluded.

[redacted]

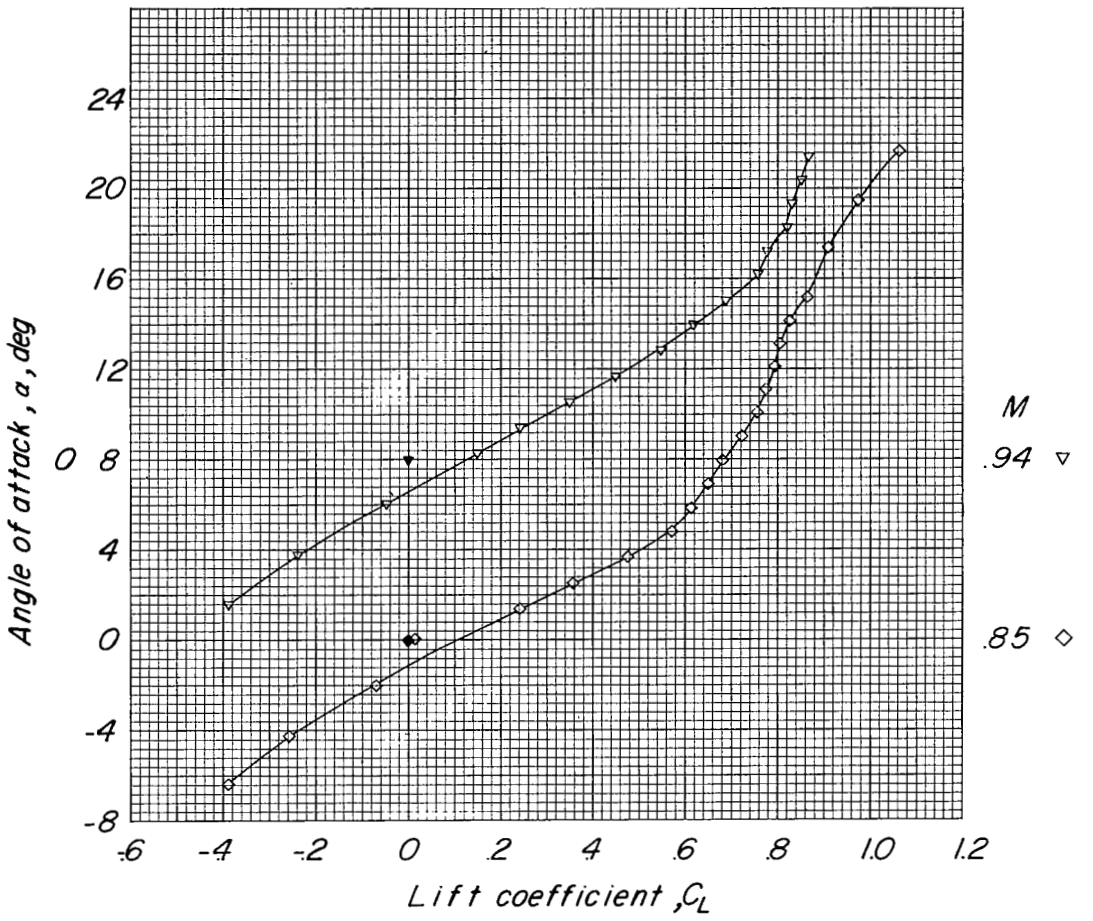

(a) α against C_L.

Figure 13.- Aerodynamic characteristics of a 1/16-scale model of the Douglas D-558-II airplane with stores B plus 7.6-percent pylons. $i_t = 0^\circ$.

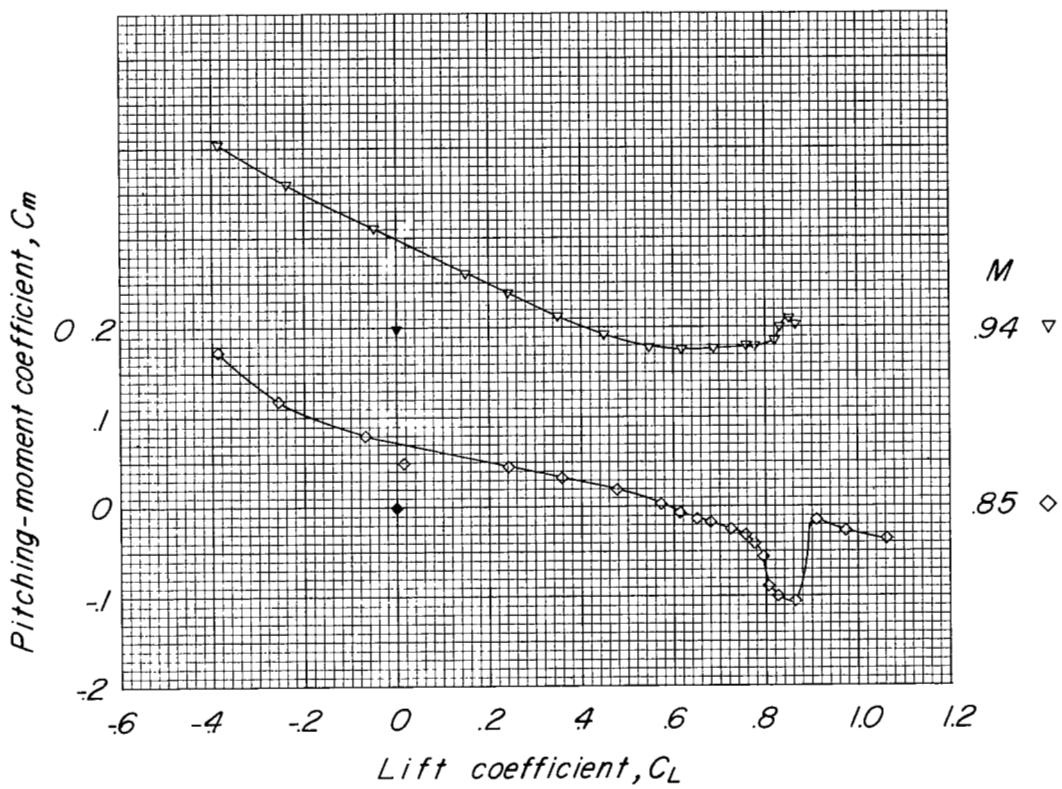

(b) C_m against C_L.

Figure 13.- Continued.

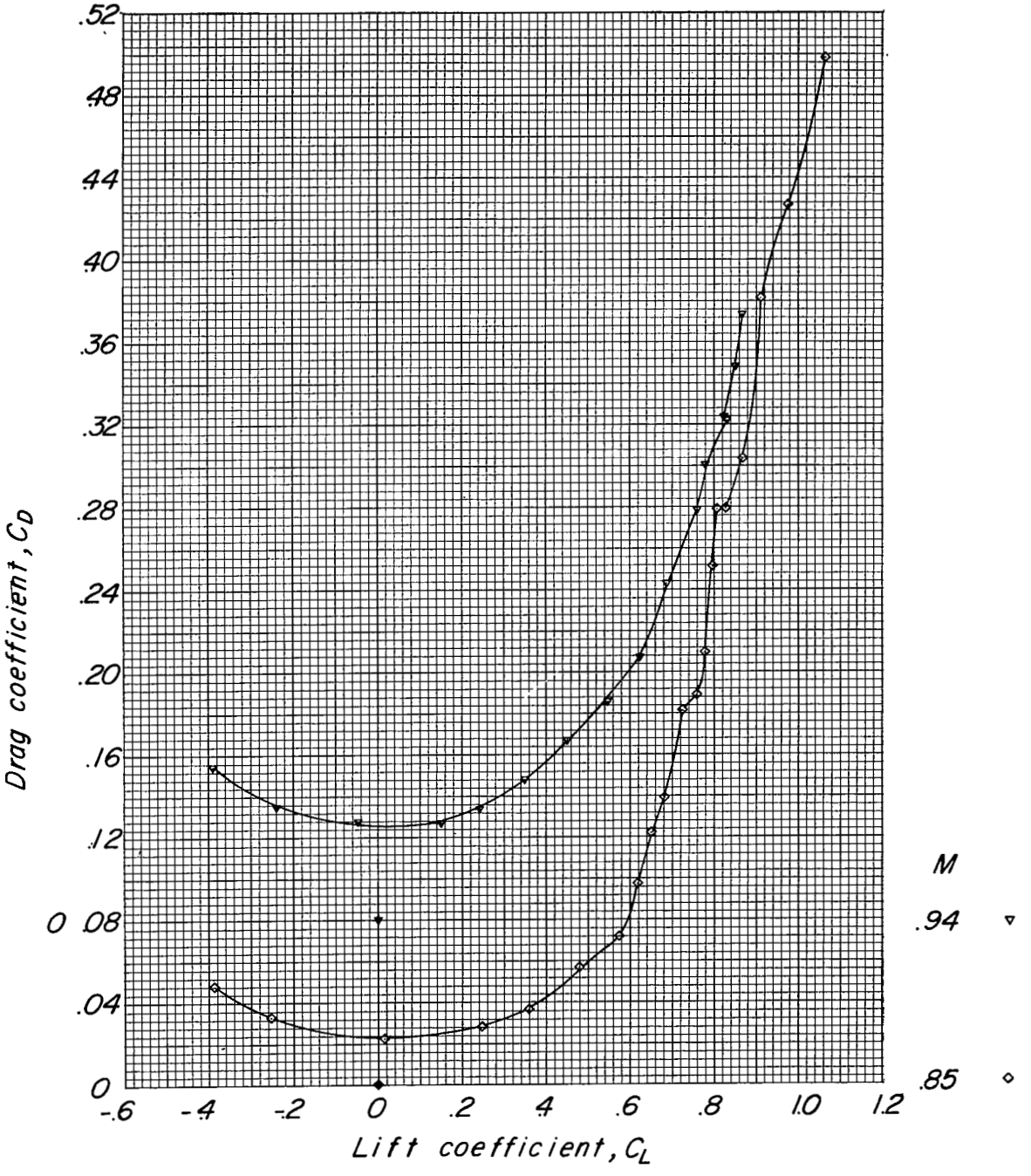

(c) C_D against C_L.

Figure 13.- Concluded.

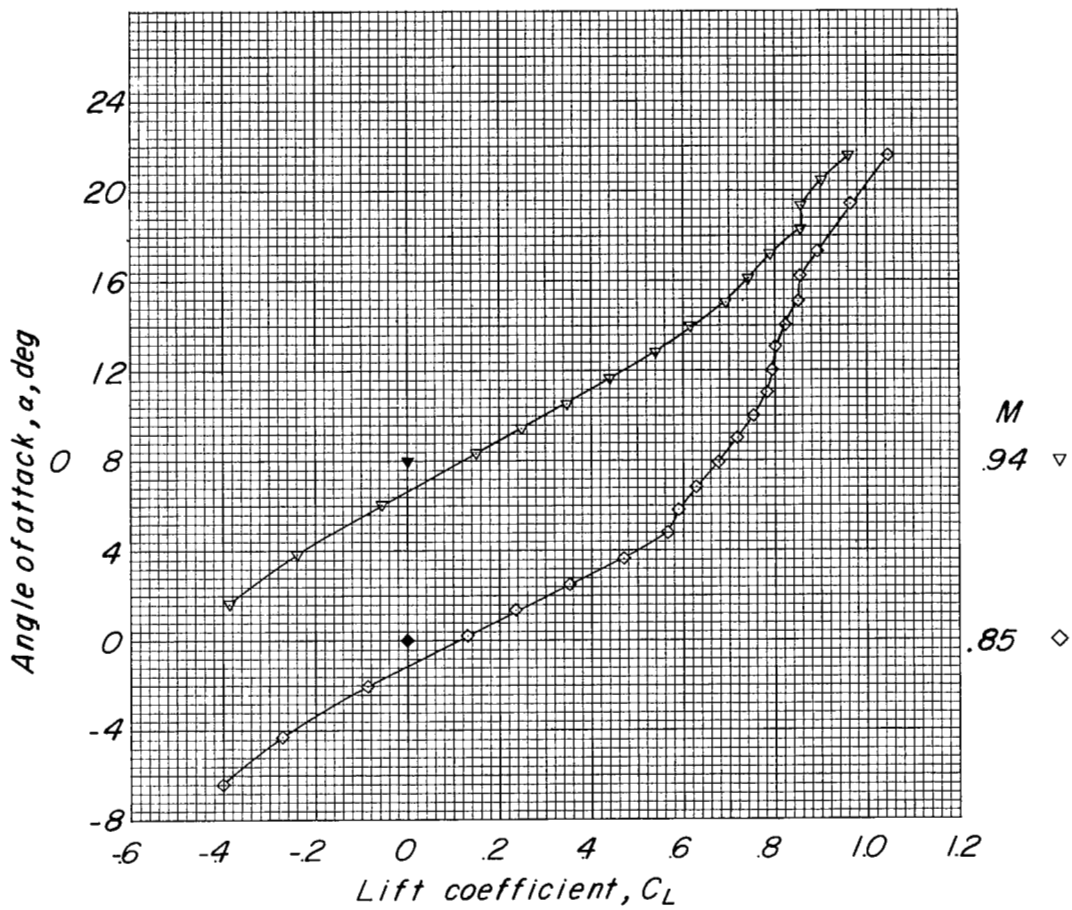

(a) α against C_L.

Figure 14.- Aerodynamic characteristics of a 1/16-scale model of the Douglas D-558-II airplane with stores C plus 7.6-percent pylons. $i_t = 0^\circ$.

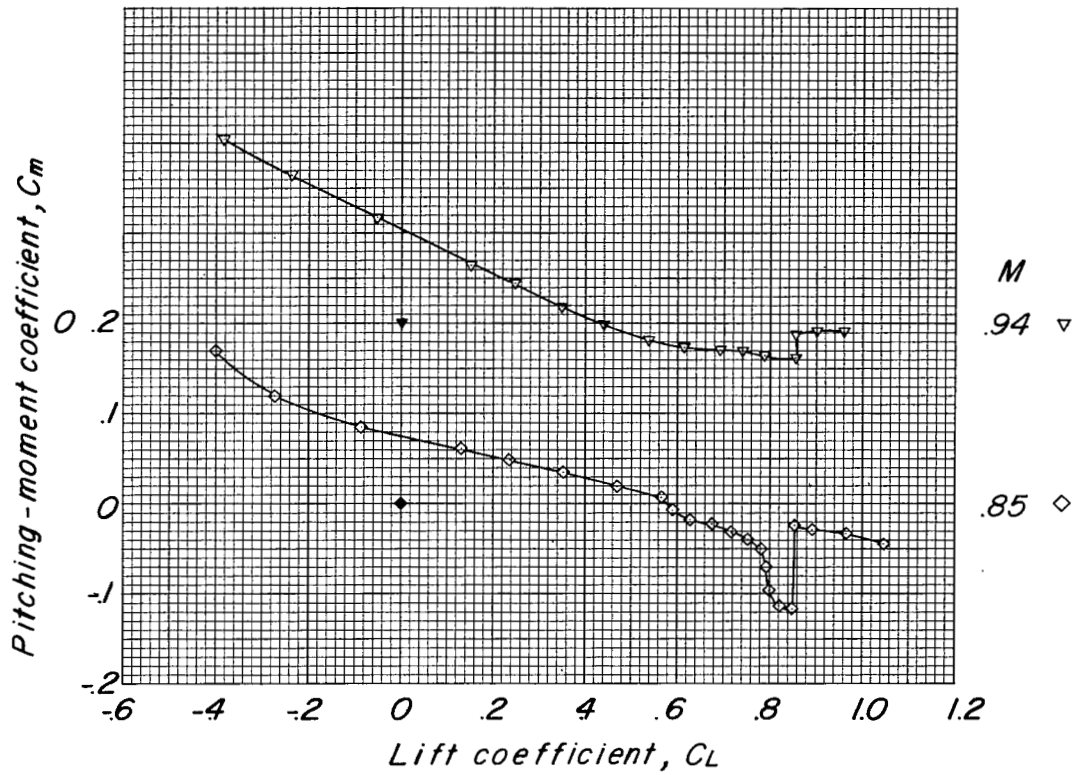

(b) C_m against C_L.

Figure 14.- Continued.

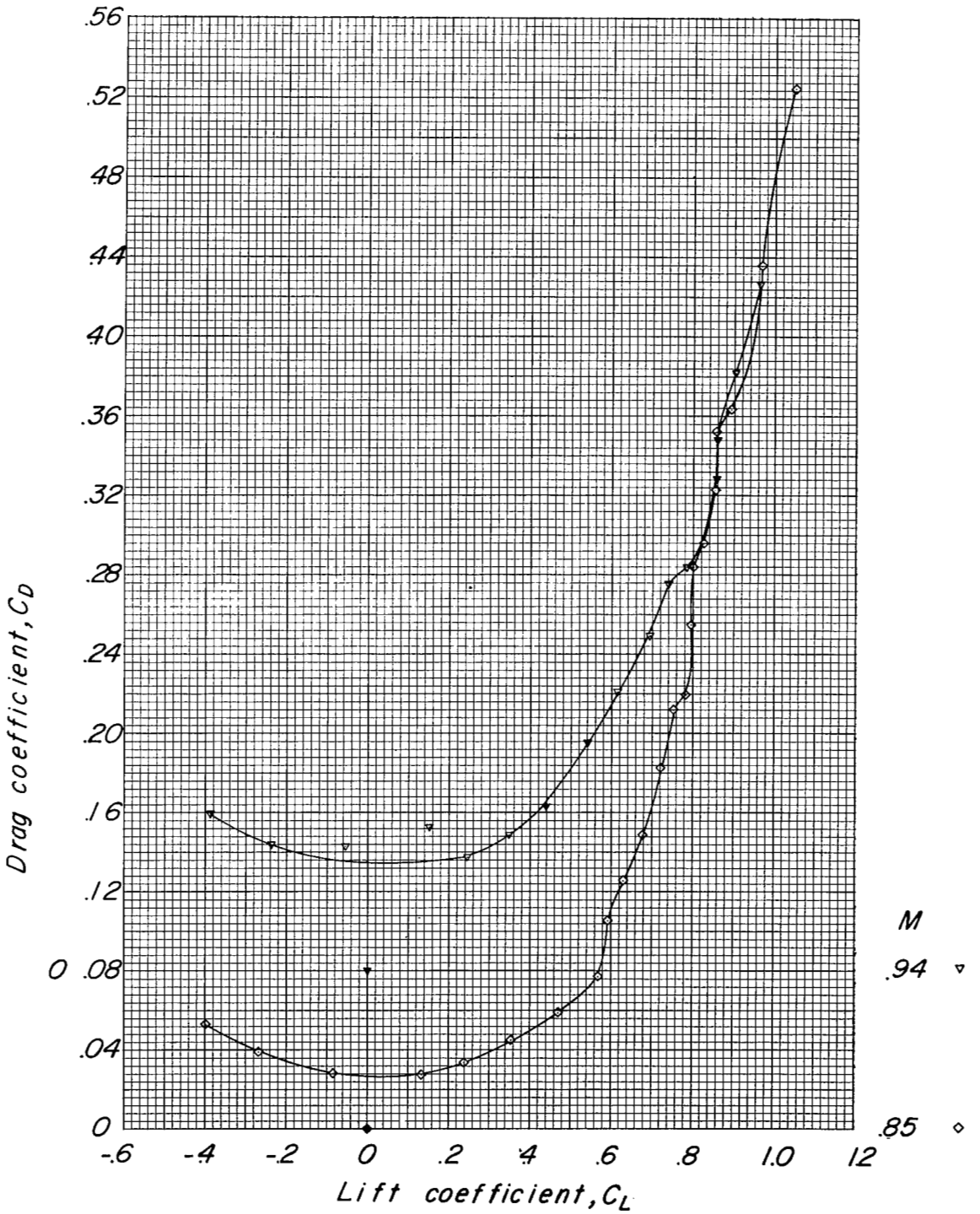

(c) C_D against C_L.

Figure 14.- Concluded.

[redacted]

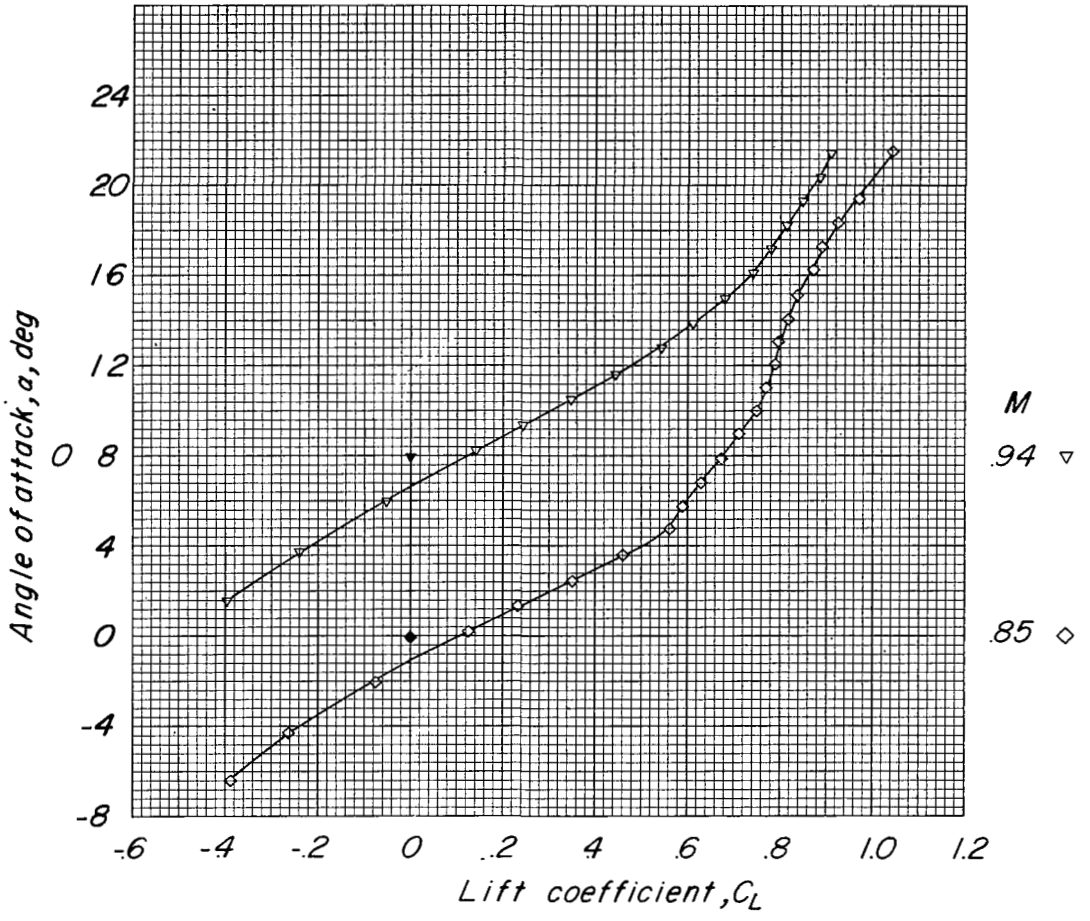

(a) α against C_L.

Figure 15.- Aerodynamic characteristics of a 1/16-scale model of the Douglas D-558-II airplane with stores D plus 7.6-percent pylons. $i_t = 0^\circ$.

[redacted]

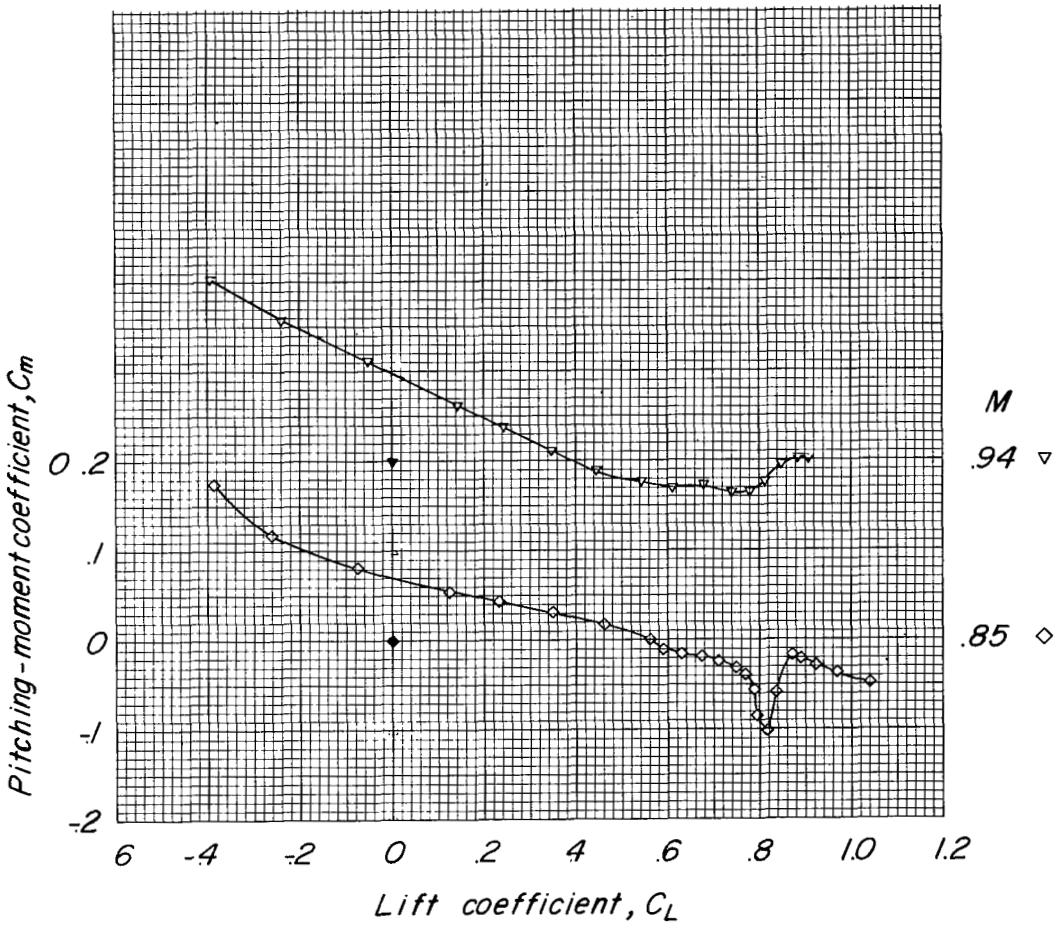

(b) C_m against C_L.

Figure 15.- Continued.

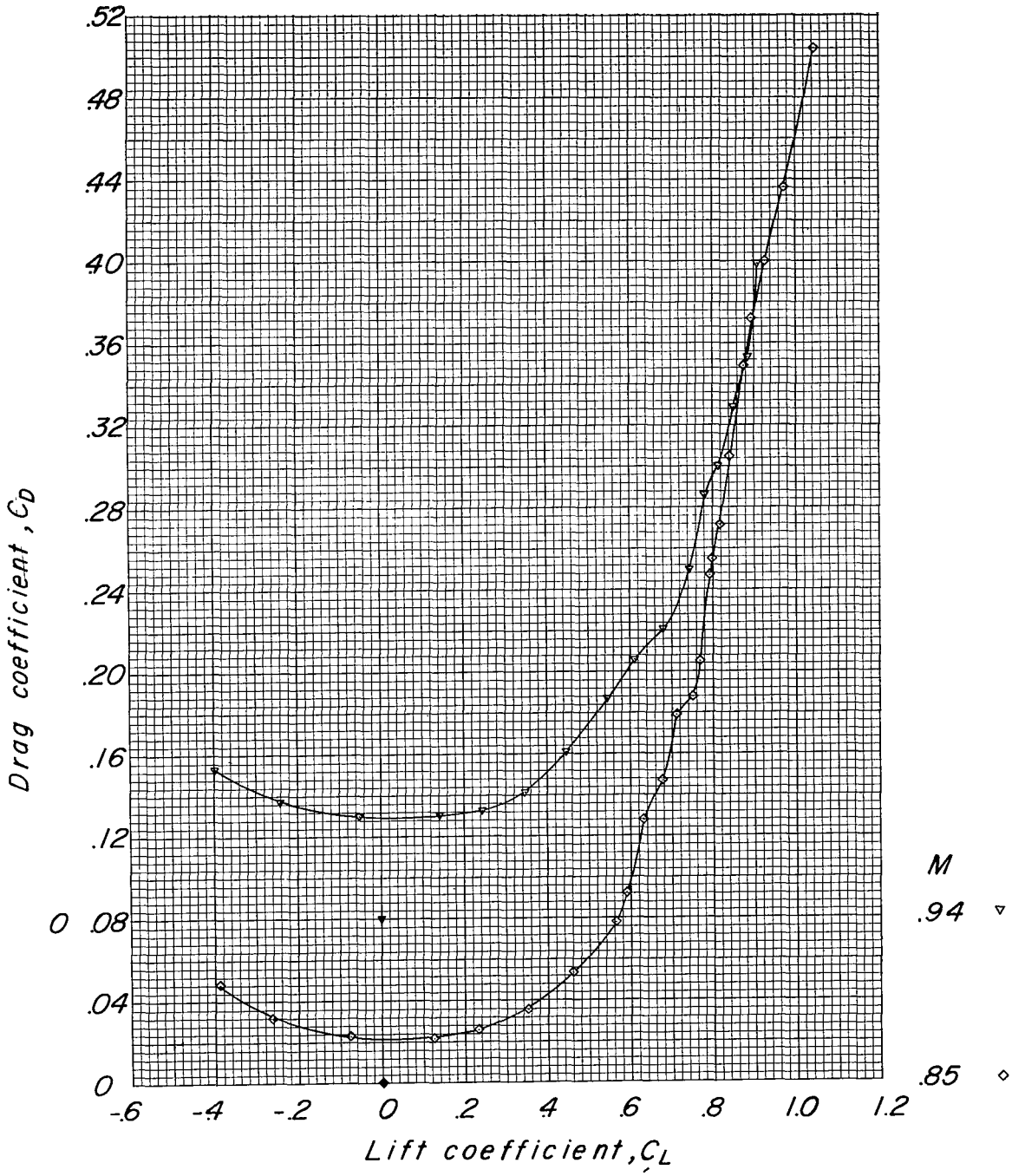

(c) C_D against C_L.

Figure 15.- Concluded.

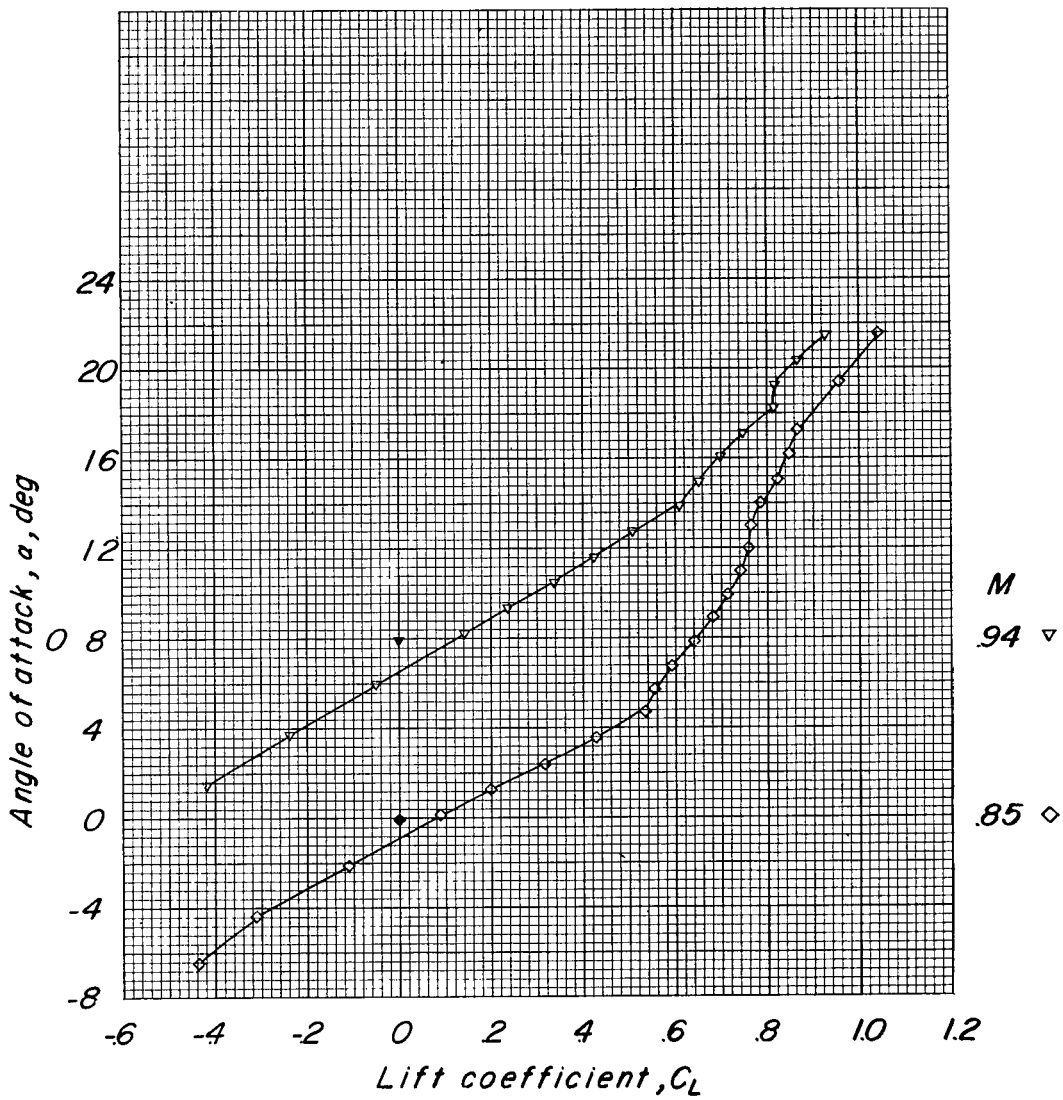

(a) α against C_L.

Figure 16.- Aerodynamic characteristics of a 1/16-scale model of the Douglas D-558-II airplane with stores E plus 7.6-percent pylons. $i_t = 0^\circ$.

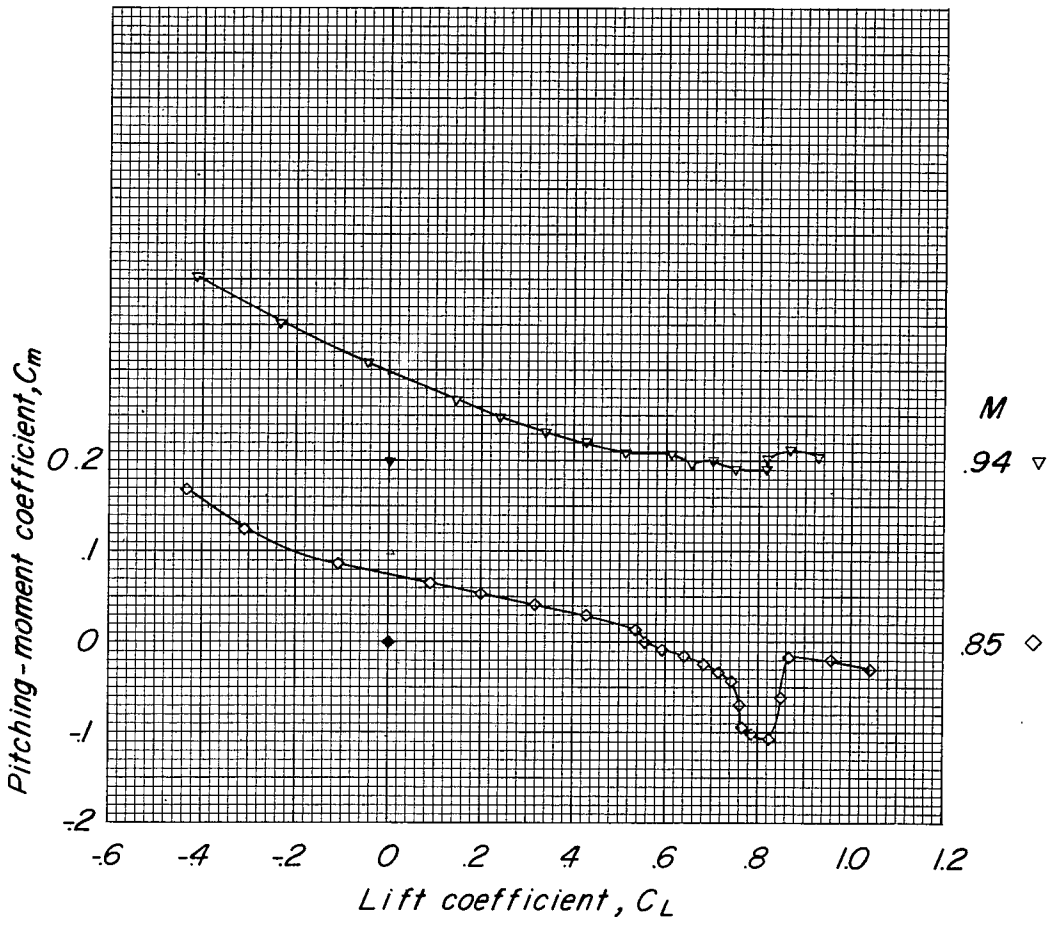

(b) C_m against C_L.

Figure 16.- Continued.

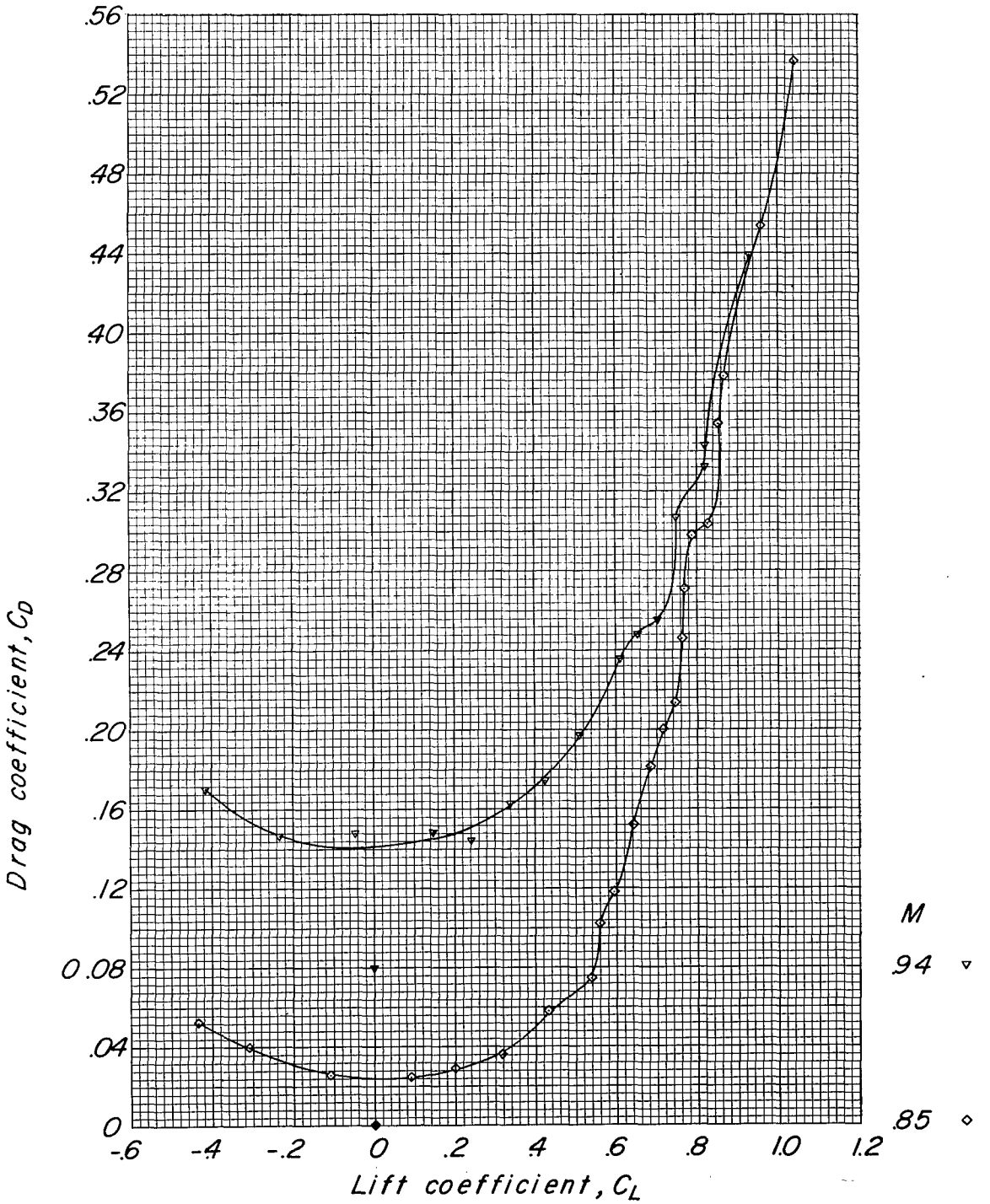

(c) C_D against C_L.

Figure 16.- Concluded.

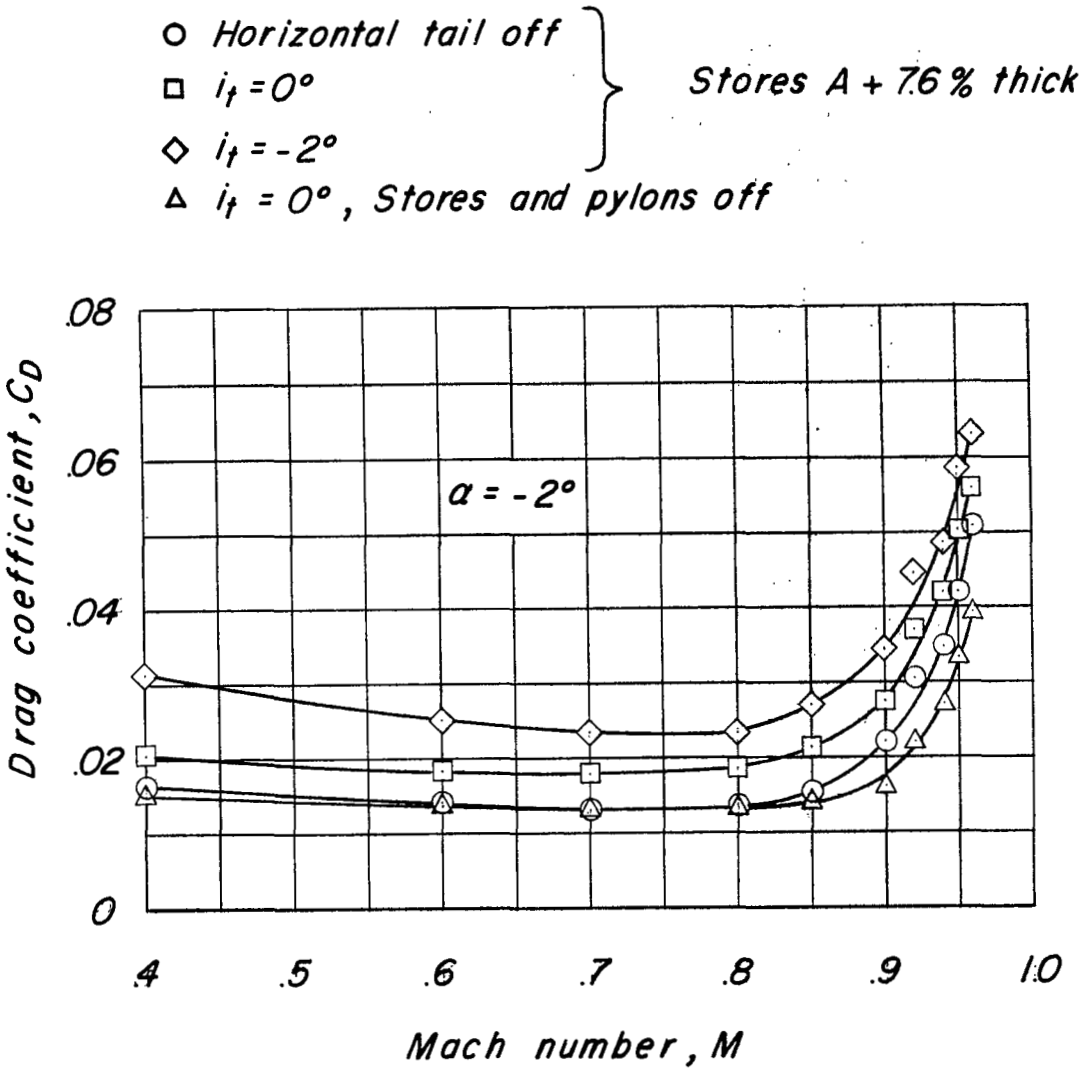

Figure 17.- Effect of the horizontal tail on the drag characteristics of a 1/16-scale model of the Douglas D-558-II airplane with stores A plus 7.6-percent pylons.

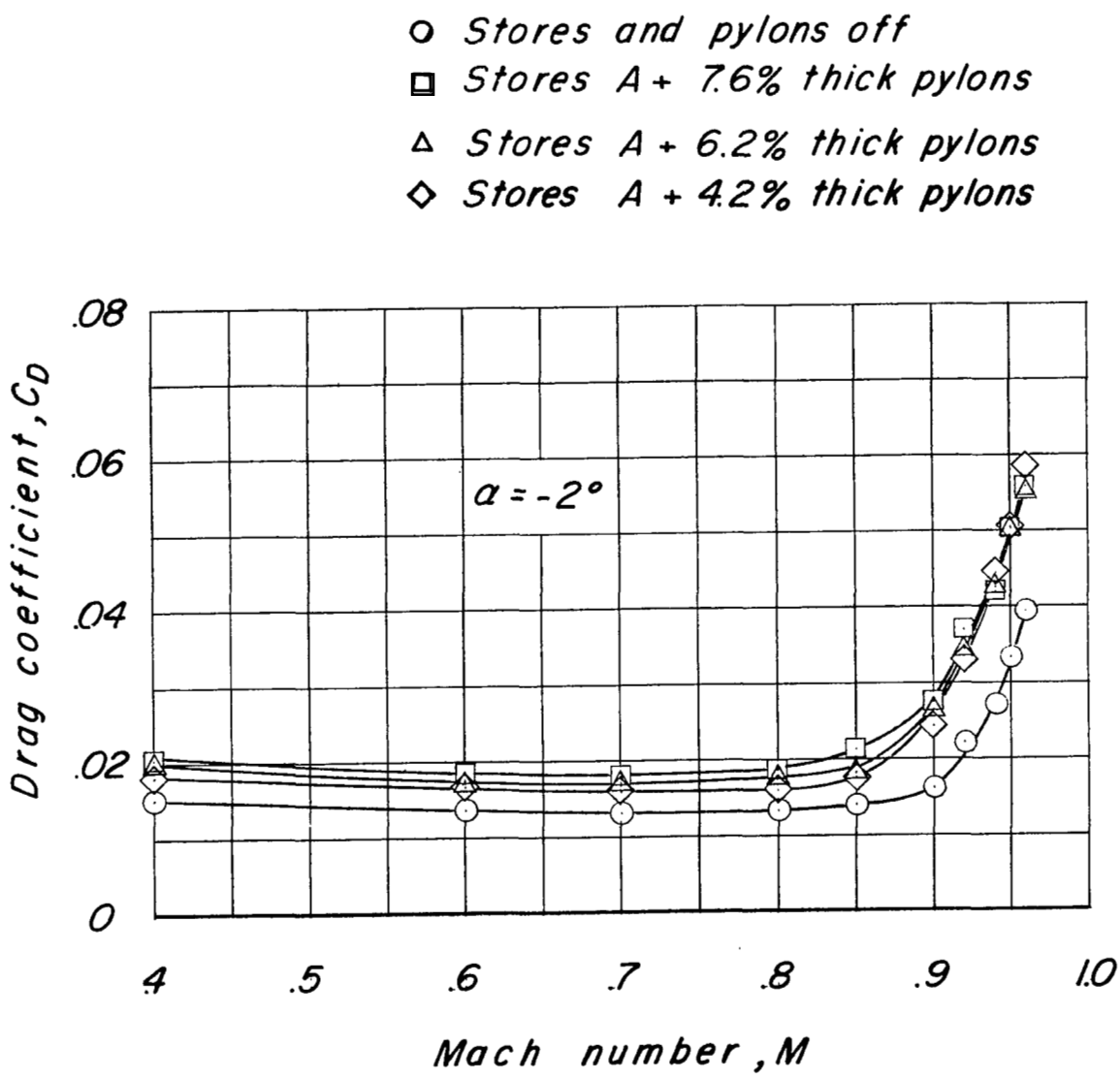

Figure 18.- Effect of pylon thickness on the drag characteristics of a 1/16-scale model of the Douglas D-558-II airplane with the short-cylinder stores A. $i_t = 0^\circ$.

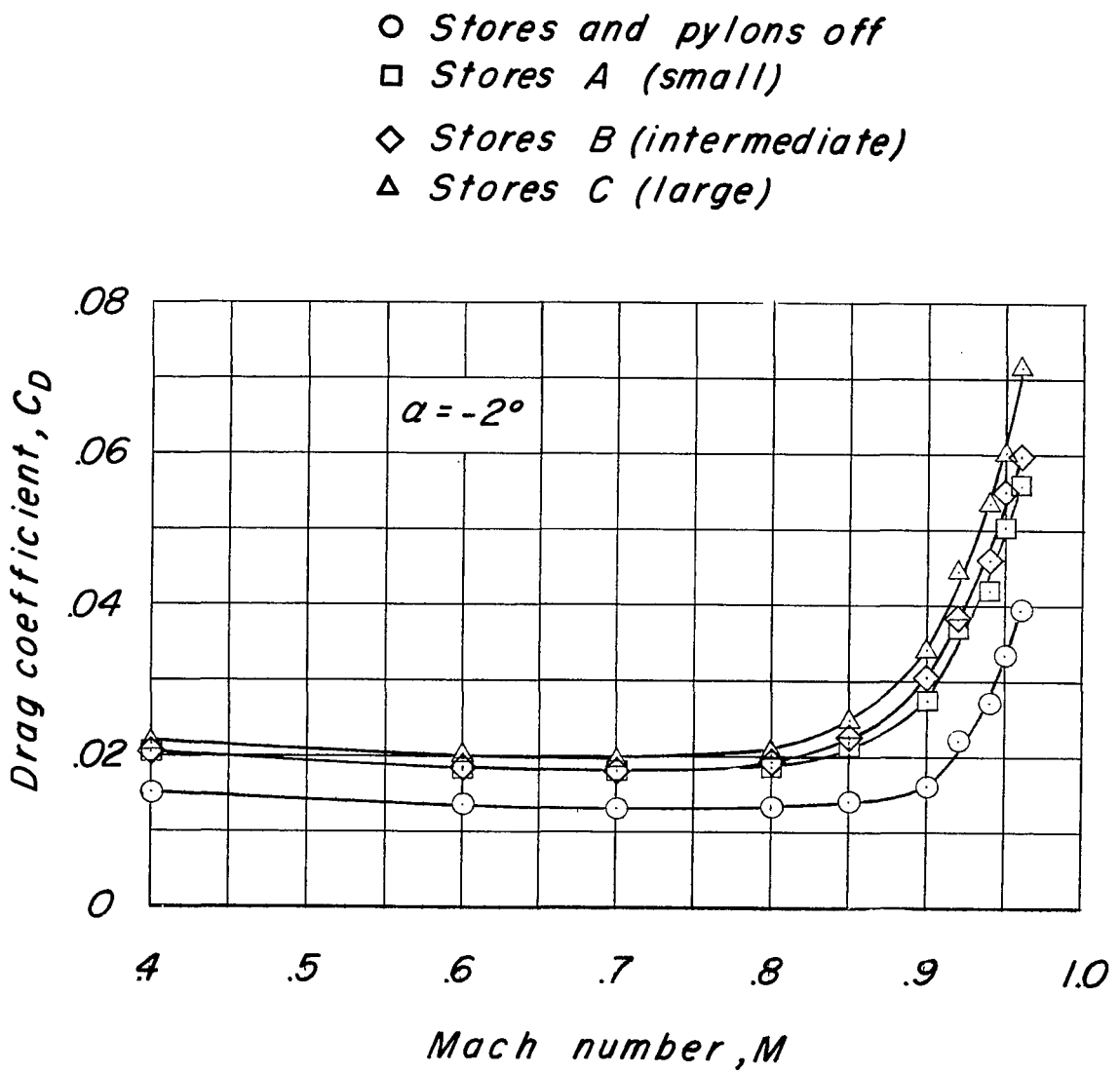

(a) Short-cylinder shape.

Figure 19.- Effect of store size on the drag characteristics of a 1/16-scale model of the Douglas D-558-II airplane with 7.6-percent pylons. $i_t = 0^\circ$.

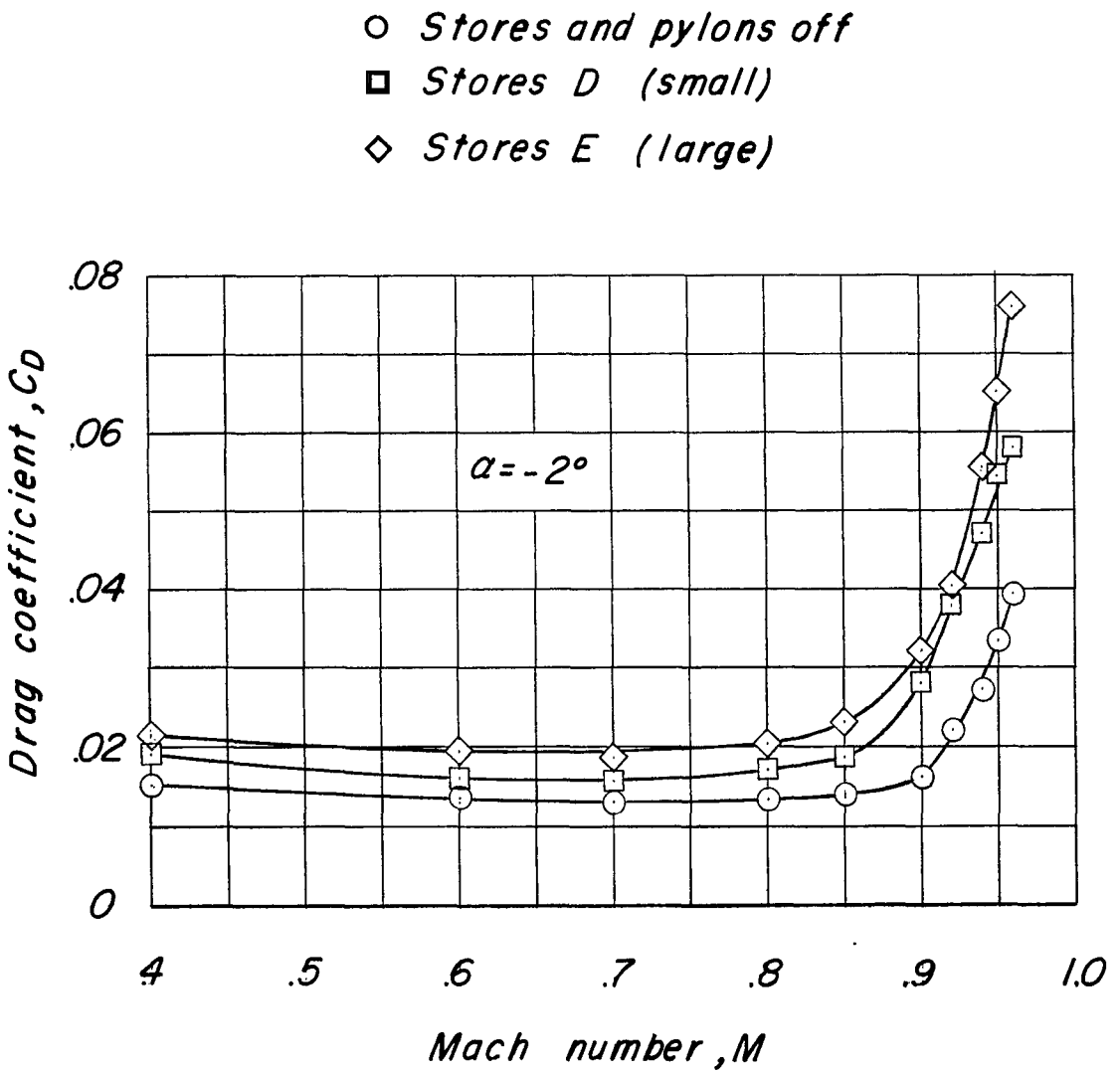

(b) Long-cylinder shape.

Figure 19.- Concluded.

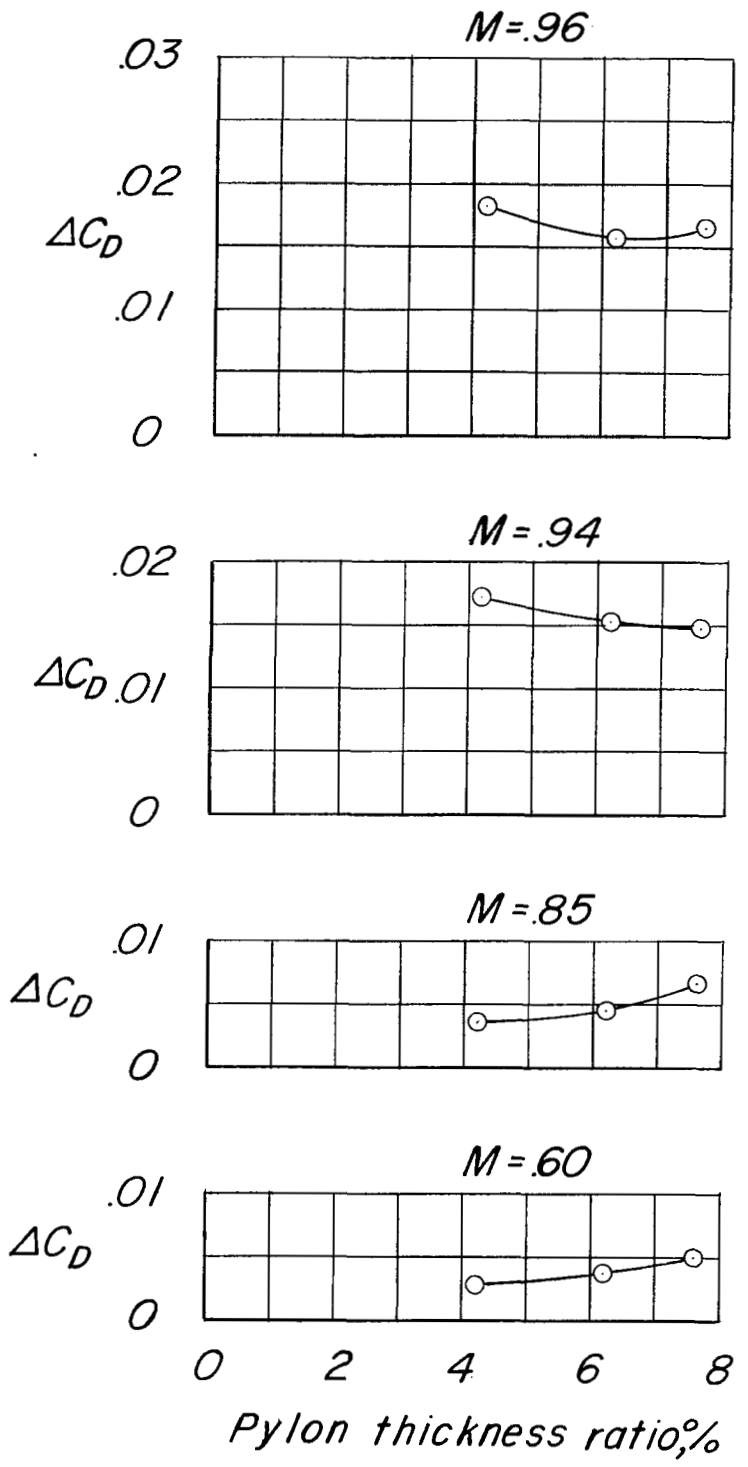

Figure 20.- Effect of pylon thickness ratio on the installation drag coefficient of a 1/16-scale model of the Douglas D-558-II airplane. $\alpha = -2^{\circ}$; $i_t = 0^{\circ}$.

[redacted]

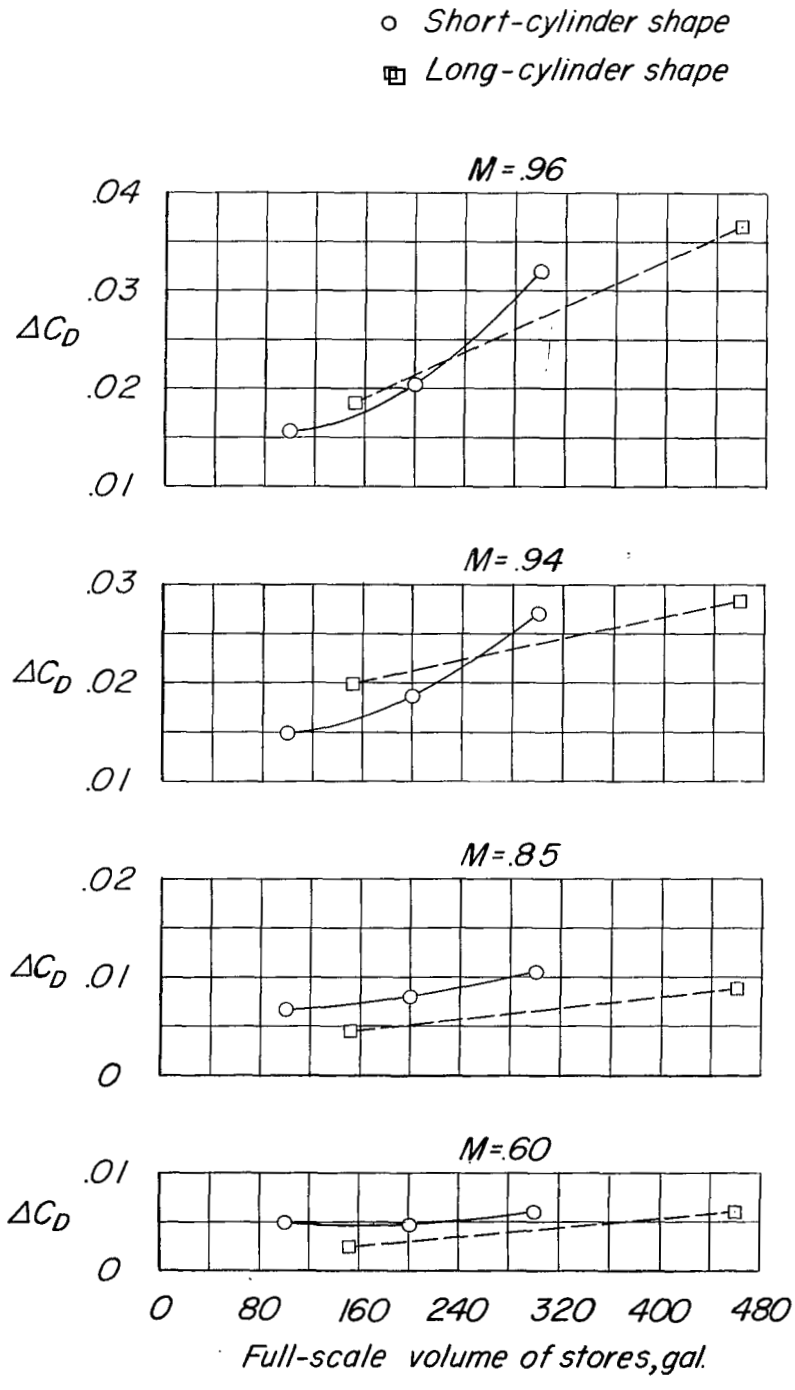

(a) Installation drag coefficient based on wing area.

Figure 21.- Effect of external store volume on the installation drag characteristics of a 1/16-scale model of the Douglas D-558-II airplane. $\alpha = -2^{\circ}$; $i_t = 0^{\circ}$.

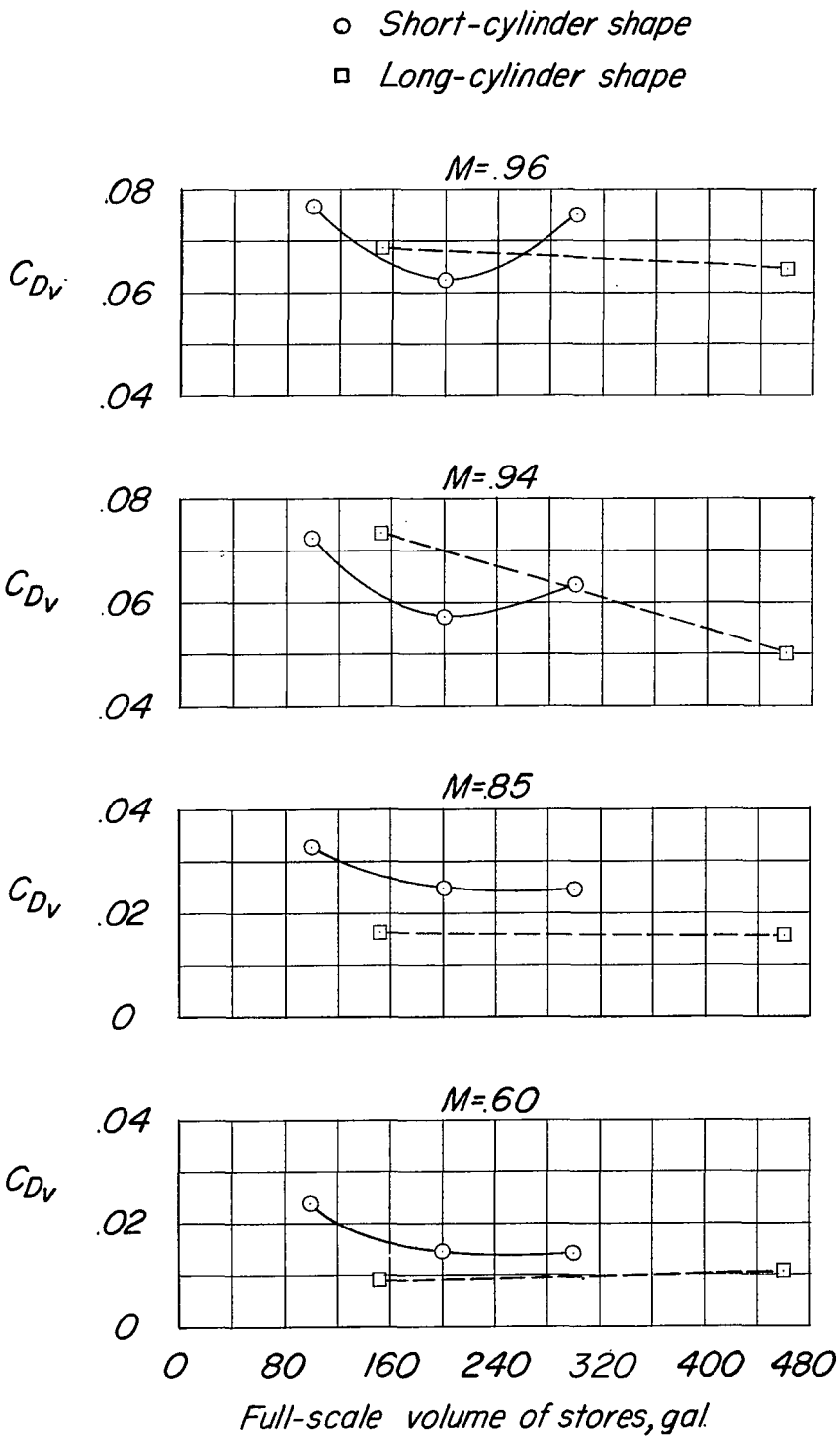

(b) Installation drag coefficient based on volume of stores.

Figure 21.- Concluded.

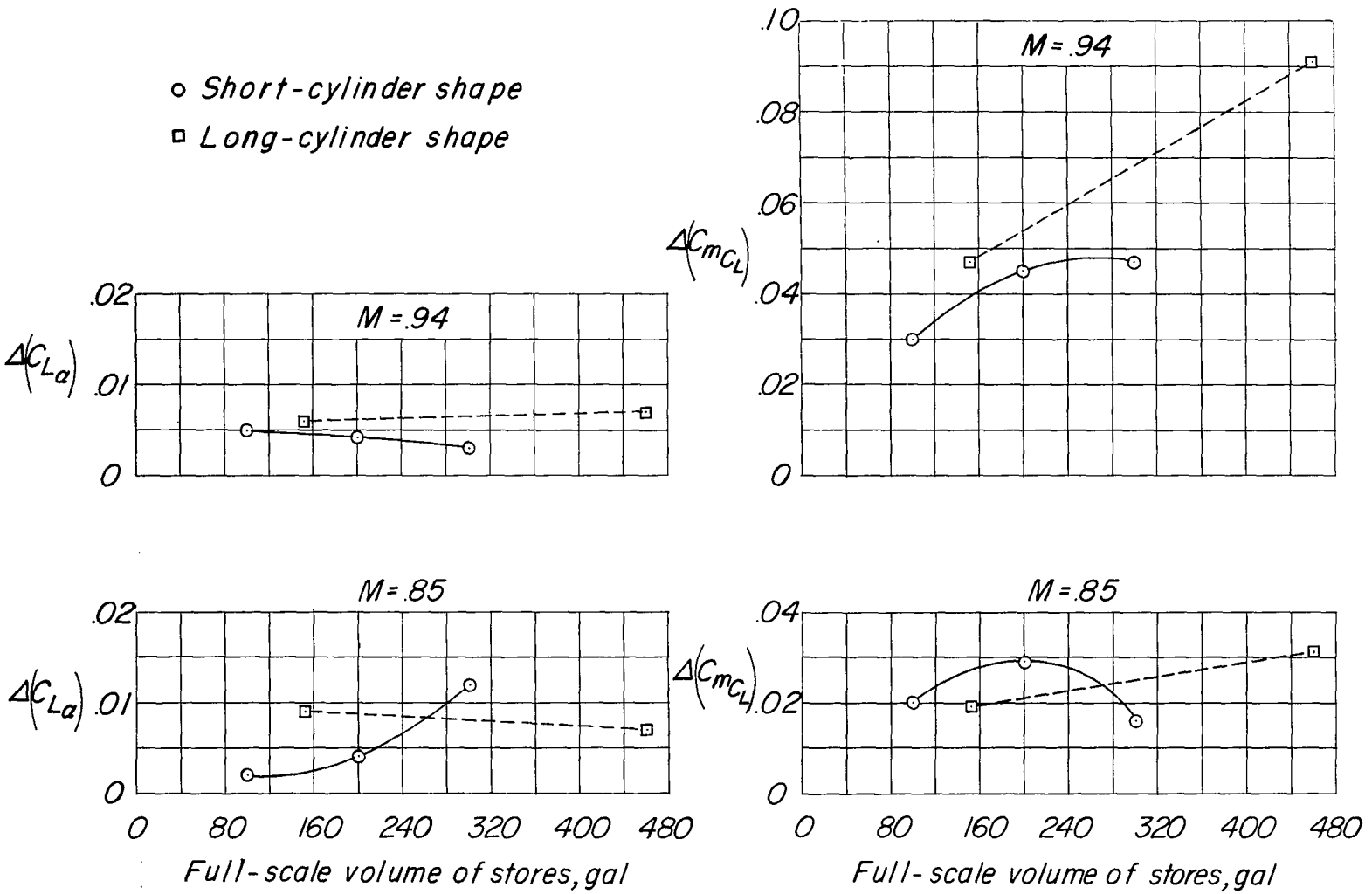

Figure 22.- Effect of external stores of several sizes on the lift-curve and pitching-moment-curve slopes of a 1/16-scale model of the Douglas D-558-II airplane. $i_t = 0^\circ$.